DOT/FAA/TC-14/26

Federal Aviation Administration
William J. Hughes Technical Center
Aviation Research Division
Atlantic City International Airport
New Jersey 08405

Advanced Fourier Transform Infrared Spectroscopy for Analyzing Damage in Aircraft Composites

October 2014

Final Report

This document is available to the U.S. public through the National Technical Information Services (NTIS), Springfield, Virginia 22161.

This document is also available from the Federal Aviation Administration William J. Hughes Technical Center at actlibrary.tc.faa.gov.

U.S. Department of Transportation
Federal Aviation Administration

NOTICE

This document is disseminated under the sponsorship of the U.S. Department of Transportation in the interest of information exchange. The U.S. Government assumes no liability for the contents or use thereof. The U.S. Government does not endorse products or manufacturers. Trade or manufacturers' names appear herein solely because they are considered essential to the objective of this report. The findings and conclusions in this report are those of the author(s) and do not necessarily represent the views of the funding agency. This document does not constitute FAA policy. Consult the FAA sponsoring organization listed on the Technical Documentation page as to its use.

This report is available at the Federal Aviation Administration William J. Hughes Technical Center's Full-Text Technical Reports page: actlibrary.tc.faa.gov in Adobe Acrobat portable document format (PDF).

Technical Report Documentation Page

1. Report No.	2. Government Accession No.	3. Recipient's Catalog No.
DOT/FAA/TC-14/26		

4. Title and Subtitle	5. Report Date
ADVANCED FOURIER TRANSFORM INFRARED SPECTROSCOPY FOR ANALYZING DAMAGE IN AIRCRAFT COMPOSITES	October 2014
	6. Performing Organization Code
7. Author(s)	8. Performing Organization Report No.
Alan Rein	
9. Performing Organization Name and Address	10. Work Unit No. (TRAIS)
Agilent Technologies 2850 Centerville Road Wilmington, DE 19808	
	11. Contract or Grant No.
12. Sponsoring Agency Name and Address	13. Type of Report and Period Covered
U.S. Department of Transportation Federal Aviation Administration 950 L'Enfant Plaza North, S.W. Washington, DC 20024	Final Report
	14. Sponsoring Agency Code
	AFS-300

15. Supplementary Notes

The Federal Aviation Administration William J. Hughes Technical Center Aviation Research Division COR was David Westlund.

16. Abstract

Aircraft employing composites require advanced nondestructive testing technology to ensure the integrity of the materials of construction. One of the variables that can potentially impact aircraft composites is thermal stress, which can lead to oxidation of the polymeric substrate of the matrix, and, in turn, potentially lead to cracks and delamination.

Because composites are predominantly comprised of organic materials, analytical instrumentation can potentially provide insight into changes occurring at the molecular level that are deleterious to composite integrity. With the recent availability of portable and mobile analytical instruments, the opportunity arises to develop new methods for nondestructively detecting chemical changes in aircraft composites directly where needed, on the aircraft, whether in manufacturing or during routine maintenance.

This project determines the ability and effectiveness of a handheld Fourier Transform Infrared Spectroscopy (FTIR) analyzer to detect incipient thermal induced damage in aircraft composites. Changes in the composite as a function of exposure time and intensity are analyzed by the hand-held FTIR analyzer, a process that compares favorably to more established nondestructive inspection techniques. Physical and mechanical tests benchmark the changes in strength in the composite coupons as a function of temperature and time of exposure; the results from these mechanical strength measurements correlate quite well with the FTIR spectroscopic data. An appropriate design of experiment ensures that the range of exposures is statistically relevant and representative of potential real-world situations that composite-based aircraft may experience.

17. Key Words	18. Distribution Statement
Composites, Damage, Inspection, Fourier Transform Infrared Spectroscopy, Nondestructive inspection	This document is available to the U.S. public through the National Technical Information Service (NTIS), Springfield, Virginia 22161. This document is also available from the Federal Aviation Administration William J. Hughes Technical Center at actlibrary.tc.faa.gov.

19. Security Classif. (of this report)	20. Security Classif. (of this page)	21. No. of Pages	22. Price
Unclassified	Unclassified	64	

Form DOT F 1700.7 (8-72) Reproduction of completed page authorized

ACKNOWLEDGEMENTS

Important contributions to this work were made by Paul Shelley (Technical Fellow, The Boeing Company), Paul Vahey (Research Chemist, The Boeing Company), Dennis Roach (Senior Scientist, Airworthiness Assurance NDI Validation Center), Paul Swindell (Research Engineer, Federal Aviation Administration (FAA)), David Galella (Project Engineer, FAA), Dirk Heider (Professor, University of Delaware Center for Composite Materials (CCM)), Joseph Deitzel (Research Associate, University of Delaware CCM), Pit Schulze (Composites Test Engineer, University of Delaware CCM), Steven Donahue (Technical Manager, Agilent Technologies, formerly A2 Technologies), John Seelenbinder (Product Manager, Agilent Technologies), Frank Higgins (Applications Engineer, Agilent Technologies), and Alan Rein (Business Development Manager, Agilent Technologies).

TABLE OF CONTENTS

		Page
EXECUTIVE SUMMARY		xii
1.	INTRODUCTION	1
1.1	Background	1
1.2	Objectives	1
1.3	FTIR Spectroscopy	2
2.	APPROACH	3
2.1	Overall Experimental Concept	3
2.2	Composite Material	3
2.3	The DoE	3
2.4	Heat Exposure Process	5
2.5	FTIR Measurements	10
2.6	The SBS Measurements	13
2.7	Ultrasonic Measurements	16
3.	RESULTS AND DISCUSSION	16
3.1	Mechanical Tests	16
3.2	The IR Spectra of Heat-Treated Composite	20
3.3	Dependence of Spectra Carbon Fiber/Resin Ratio	21
3.4	Relationship Between Changes in Spectra and Mechanical Strength of Composite	23
3.5	The PLS Correlation of FTIR Spectra and SBS Data	23
3.6	Neural Net Analysis of FTIR Data	26
3.7	Use of ExoScan Analyzer for Mapping Surface of Damaged Composite Panel	28
3.8	Thermal Damage – Additional Studies in the “Transition” Range	34
3.9	BMS8-276 4″ Coupons	34
3.10	BMS8-256 4″ Coupons	39
3.11	Ultrasound and Microscopy	45

4. SUMMARY 49

5. CONCLUSIONS 51

6. REFERENCES 52

LIST OF FIGURES

Figure		Page
1	The DoE	4
2	Received Composite Coupons in Drying Pan	6
3	Temperature-Monitoring Setup	7
4	Schematic of Coupon Mounting and Thermocouple (TC) Locations	7
5	Coupon Clamped in Binder Clip	8
6	Clips Mounted on Steel Rod and Profiles	8
7	Example of Temperature History During Thermal Exposure of Composite Coupons Suspended in Oven	10
8	Agilent Technologies 4100 ExoScan System Mounted in Docking Station for Measurement of Thermal Damage in Composite Coupons	11
9	ASTM D2344 Setup on Instron 4484	14
10	Detailed View of Coupon Mounting in Test Fixture	14
11	The SBS Strength for Both Sets of BMS8-276 Coupons	19
12	The SBS Strength for Both Sets of BMS8-256 Coupons	19
13	Specular Reflectance IR Spectra of Composite as a Function of Temperature and Time Exposure	20
14	The IR Spectra of the Outer Surface of the Composite Coupon via Specular and Diffuse Reflectance	21
15	Comparison of Specular and Diffuse Reflectance IR Spectra for Sanded Composite	22
16	Neural Network Architecture Used for the Evaluation of Thermally Damaged Composite Coupons	27
17	Neural Network Toolbox Output for Summarizing Predicted vs. Actual Results Based on FTIR Data Independent of SBS Results	28
18	Thermocouple Location	29

19	Composite Panel Lined With Tape	29
20	Setup and Markings on Tape	30
21	Composite Panel With Tranparencies	30
22	ExoScan Fitted With Stand	31
23	ExoScan Closeup	31
24	Laser Levels	32
25	ExoScan Laser Positioning	32
26	Contour Maps for Thermal Damage as a Function of Distance for Panels Exposed to Increasing Levels of Thermal Stress	33
27	Thermal Damage as a Function of Position for Composite Panel Exposed to Highest Levels of Heat	33
28	Force vs. Temperature/Time Combinations for BMS8-276	35
29	The IR Spectra for BMS8-276	36
30	Cluster Analysis of Spectral Data for BMS8-276	37
31	Spectra Clustering of Low, Medium, and High Damage Within the Dataset for 4″ BMS8-276 Coupons	37
32	Spectra of Composite Exposed to 490°F for Progressive Times – 30 Minutes, 50 Minutes, 70 Minutes, 90 Minutes, and 120 Minutes	38
33	Spectra of 4″ BMS8-276 Coupons Exposed to 490°F for Progressive Times – 30 Minutes, 50 Minutes, 70 Minutes, 90 Minutes, and 120 Minutes Overlayed With Minimum andMaximum Thermally Exposed 1″ Coupons	39
34	Force vs. Temperature/Time Combinations for BMS8-256	41
35	The IR Spectra for 4″ BMS8-256 Coupons	42
36	Cluster Analysis of Spectral Data for 4″ BMS8-256 Coupons	43
37	Second Derivative IR Spectra Demonstrating Clustering of Low, Medium, and High Exposure in the 4″ BMS8-256 Coupons: 430°F, 50 Minutes (red); 445°F, 120 Minutes (blue); 475°F, 120 Minutes (green)	43

38 Second Derivative Spectra of 4″ BMS8-256 Composite Coupons Exposed to 460°F for Progressive Times – 30 Minutes, 50 Minutes, 70 Minutes, 90 Minutes, and 120 Minutes 44

39 Second Derivative Spectra of 4″ BMS8-256 Composite Coupons Exposed to 460°F for Progressive Times – 30 Minutes (cyan), 50 Minutes (blue), 70 Minutes (green), 90 Minutes (black), and 120 Minutes (orange) Overlayed With Earlier 1″ Minimum (purple) and Maximum (red) Thermally Damaged Coupons 45

40 A-Scan Measurement of Composite Prior to Thermal Exposure 46

41 A-Scan Measurement of Composite After Thermal Exposure 46

42 A-Scan Measurement of Composite After Thermal Exposure 47

43 C-Scan Measurements of Composite Coupons: C13 Exposed to 385°F for 198 Minutes; C19 Exposed to 415°F for 510 Minutes; C20 Exposed to 445°F for 510 Minutes 47

44 Microscopic Evalution of BMS8-256 as a Funtion of Increasing Temperature and Exposure Time 48

45 Summary of SBS, Ultrasound, and Microscopic Analysis of BMS8-256 Coupons as a Function of Temperature/Time Exposures 48

46 Summary of SBS, Ultrasound, and Microscopic Analysis of BMS8-276 Coupons as a Function of Temperature/Time Exposures 49

LIST OF TABLES

Table		Page
1	Thermal Damage Study - Temperature and Time Levels	4
2	Temperature and Time Exposures for Composite Thermal Damage Studies Based on DoE	5
3	Example Thermal Exposure Matrix for BMS8-256	9
4	Order for FTIR Measurements of BMS8-276 Composite Coupons	12
5	Example of Coupon Dimensions for BMS8-276	14
6	Average Absolute and Relative SBS Strength of BMS8-276	17
7	Average Absolute and Relative SBS Strength of BMS8-256	18
8	Results of Spectra/Mechanical Strength Correlation for BMS8-276 Evaluation Set	24
9	Results of Spectra/Mechanical Strength Correlation for BMS8-256 Evaluation Set	24
10	Results of Spectra/Mechanical Strength Correlation for Sanded BMS8-256 Evaluation Set	25
11	Results of Spectra/Mechanical Strength Correlation for Unsanded BMS8-256 Evaluation Set as Measured by Specular Reflectance	25
12	Results of Spectra/Mechanical Strength Correlation for Sanded BMS8-256 Evaluation Set as Measured by Diffuse Reflectance	26
13	The SBS Data for 4″ BMS8-276 Coupons, Which Were Analyzed at AANC and Then Cut Into 1″-Size for SBS Analysis at CCM	34
14	The SBS Data for BMS8-256 4″ Coupons, Which Were Analyzed at AANC and Then Cut Into 1″ Size for SBS Analysis at CCM	40

LIST OF ACRONYMS

A/N	Absorbance to noise
AANC	Airworthiness Assurance NDI Validation Center
ASTM	American Society for Testing and Materials
BMS	Boeing Material Specification
CCM	Center for Composite Materials
DoE	Design of Experiment
FTIR	Fourier Transform Infrared Spectroscopy
IR	Infrared
NDI	Nondestructive inspection
NDT	Nondestructive testing
PLS	Partial least squares
SBS	Short beam shear
TC	Thermocouple
TTU	Through-transmission ultrasound
UV	Ultraviolet radiation

EXECUTIVE SUMMARY

Aircraft employing composite materials in their construction require advanced nondestructive testing technology to ensure the integrity of the materials. One of the variables that can potentially impact aircraft composite materials is thermal stress, which can lead to the oxidation of the polymeric substrate of the matrix and, in turn, potentially lead to cracks and delamination.

Because composites are predominantly comprised of organic materials, analytical instrumentation can potentially provide insight into changes occurring at the molecular level that are deleterious to composite integrity. With the recent availability of portable and mobile analytical instruments, the opportunity arises to develop new methods for nondestructively detecting chemical changes in aircraft composites, directly where needed on the aircraft, whether in manufacturing or during routine maintenance.

This project determines the ability and effectiveness of a handheld Fourier Transform Infrared Spectroscopy (FTIR) analyzer to detect incipient thermal induced damage in aircraft composites. Changes in the composite as a function of exposure time and intensity are analyzed by the hand-held FTIR analyzer, a process that compares favorably to more-established nondestructive inspection techniques. Physical and mechanical tests benchmark the changes in strength in the composite coupons as a function of temperature and time of exposure; the results from these mechanical strength measurements correlate quite well with the FTIR spectroscopic data. An appropriate design of experiment ensures that the range of exposures is statistically relevant and representative of potential real-world situations that composite-based aircraft might experience.

1. INTRODUCTION.

1.1 BACKGROUND.

The prospect of using composite materials to reduce airframe weight (and, thus, enable greater fuel economy and lower operating costs) has led to its accelerated adoption in commercial aircraft. The anticipated increased use of composites presents new challenges in maintaining safe flying conditions. In fact, there have already been calls for improving the inspection process for composite materials [1]. While all aircraft are subject to environmental damage, composite materials are susceptible to environmental damage that is different from that which traditional aluminum materials suffer. The resin component of the composite consists of organic molecules, which are susceptible to the effect of a number of external stressors, such as heat, cold, moisture, ultraviolet (UV) light, and exposure to chemicals. Analyzing the effect of these environmental stressors on in-service composite-based aircraft requires new techniques and strategies.

In 1990, Oak Ridge National Laboratory published a report [2] on several spectroscopic techniques for determining the extent of heat damage on composite panels. The study revealed that diffuse reflectance Fourier Transform Infrared Spectroscopy (FTIR) and laser-induced fluorescence had the highest degrees of success, but both techniques required development of a field unit that could be used for nondestructive inspection (NDI). Late in the 1990s, a mobile FTIR system designed for the field analysis of composites was developed. However, this system weighed 20 pounds and had ergonomic limitations with respect to inspecting non-flat composites or composite locations that were less accessible.

In 2008, a 7-pound battery-powered FTIR analyzer was introduced. The ExoScan system (developed by Agilent Technologies, formerly A2 Technologies) is equipped with sampling interfaces that permit the nondestructive analysis of optically opaque materials, such as the mid-modulus, carbon fiber resin composites that are used by the aerospace industry.

On September 18, 2008, the Federal Aviation Administration awarded a 3-year research contract to A2 Technologies (now part of Agilent Technologies) to determine the value and feasibility of employing this handheld, battery-operated FTIR as a new non-destructive testing analyzer for composite-based aircraft. The collaborators on this project are A2 Technologies, the University of Delaware Center for Composite Materials (CCM), the Airworthiness Assurance NDI Validation Center (AANC) at Sandia National Labs, and The Boeing Company.

1.2 OBJECTIVES.

The main project objective is to determine if the ExoScan FTIR system can detect incipient thermal damage in aircraft composites. To accomplish this, coupons of composites used in civilian aircraft manufacture were exposed to varying temperature and time combinations.

Changes in the composite as a function of exposure time and intensity were measured by the handheld FTIR analyzer and established NDI techniques. Physical and mechanical tests were used to benchmark the changes in strength in the composite coupons; the results from these mechanical strength measurements have been correlated with the spectroscopic and NDI results. A Design of Experiment (DoE) was developed to ensure that the range of exposures was

statistically relevant and representative of potential real-world situations that composite aircraft might experience. The primary questions and objective to be investigated in this research project were:

- Does FTIR, a nondestructive surface method, detect chemical changes in composites that may relate to changes in the overall strength (a bulk property) of the composite?

- If so, can a reliable FTIR method be developed that rapidly elucidates change in composite strength induced by thermal affects? Can trained nondestructive testing (NDT) operators routinely execute the method and deliver reliable results?

- What is the relevance of FTIR as an NDI method for composites, and how does it compare to more commonly used NDI methods?

- Work with third party to calibrate and validate the ExoScan technology for use in detecting heat damage in composite-based aircraft.

1.3 FTIR SPECTROSCOPY.

FTIR spectroscopy is a widely used analytical method and FTIR spectrometers are present in virtually all industry and academic laboratories. The primary use is to provide information about molecular identity and structure as defined by patterns of characteristic absorbance bands, primarily measured in the 4000 cm^{-1} to 500 cm^{-1} (2.5–20 microns) region of the spectrum.

The position and intensity of these characteristic absorbance patterns are directly related to interatomic vibrations in the molecules and, thus, are diagnostic for the identity and quantity of specific molecules present in a sample.

An FTIR spectrometer contains an infrared (IR) source, interferometer, and IR energy detector. In its simplest form, the interferometer consists of a beamsplitter, fixed mirror, and constant-velocity moving mirror. IR radiation from the source is split into two components by the beamsplitter then recombined, passed through a sample, and delivered to the detector. The moving mirror creates a pattern of constructive and destructive interference of all the wavelengths of IR radiation simultaneously. This pattern of interferences is called the interferogram. When the radiation from the interferometer is passed through a sample, some of the wavelengths of energy are absorbed by the molecules, resulting in an altered interferogram. This molecule-specific interference pattern is then converted from the time-distance domain to the frequency domain using a Fourier transform algorithm, resulting in the familiar and characteristic IR spectrum of the sample.

2. APPROACH.

2.1 OVERALL EXPERIMENTAL CONCEPT.

- Via the DoE, expose composite materials to a range of variables (e.g., time, temperature, intensity of exposure, etc.) to induce thermal, UV, or chemical damage.

- Measure the damage using IR spectroscopy and "gold standard" NDI, as well as physical methods.

- Determine the best IR sampling method for both fiber-poor (composite surface) and fiber-rich (subsurface, via sanding) sections of composite.

- Establish correlation between IR results and data provided by NDI/physical measurements.

- Based on the above correlations, develop methods/protocol for use of IR analyzer technology by NDT technicians.

2.2 COMPOSITE MATERIAL.

The Boeing Company provided the epoxy resin composite materials for this project. Two different composites were chosen: 1) Boeing material specification (BMS) 8-276, used in the fuselage of the Boeing 787 airliner and 2) BMS8-256, used in the vertical tail fin assembly of the Boeing 777 airliner. Large panels of the composites were prepared from prepreg at Boeing. After curing, these composite panels were examined by through-transmission ultrasound (TTU) to ensure integrity. The dynamic range was 140 dB (tone-burst), using a water jet TTU scan system with 5Mhz scans. These panels were then cut into small coupons, which were approximately 0.18″ thick (24 ply) x 0.36″ wide x 1.08″ long.

Several 12″-square panels of the two composites were prepared to be used for mapping studies. These studies were intended to determine whether the FTIR system could measure the point where pristine composite ends and damaged composite begins on a larger surface and, thereby, map the extent of damage.

Additionally, sixty-three 4″ x 4″ coupons for each of the two composites were fabricated at Boeing. These coupons were used for more thorough evaluation in the transition region between undamaged and damaged composite material.

2.3 THE DoE.

Based on discussions with Boeing, a series of temperature and time levels were selected for this project (table 1), which were considered representative of actual conditions to which the composite could be exposed. The DoE (figure 1) called for 40 combinations of time and temperature exposure to generate the samples required for thoroughly evaluating the FTIR-based method for predicting thermal damage. A total of 240 coupons were prepared for each of the two composites to carry out triplicate measurement by both FTIR and the reference short beam

shear (SBS) measurements. A portion of these coupons were used for developing the calibrations that correlate the IR spectra to thermally induced mechanical damage; the remainder was used for validating the methods. Additionally, 10 coupons, each 4″ x 4″ x 0.18″, were exposed to varying time and temperature combinations to enable additional NDI tests.

Table 1. Thermal Damage Study−Temperature and Time Levels

	Levels							
Variable	1	2	3	4	5	6	7	8
Temperature (°F)	325	355	385	415	445	475	505	535
Time (minutes)	30.00	48.11	77.14	123.69	198.34	318.05	510.00	n/a

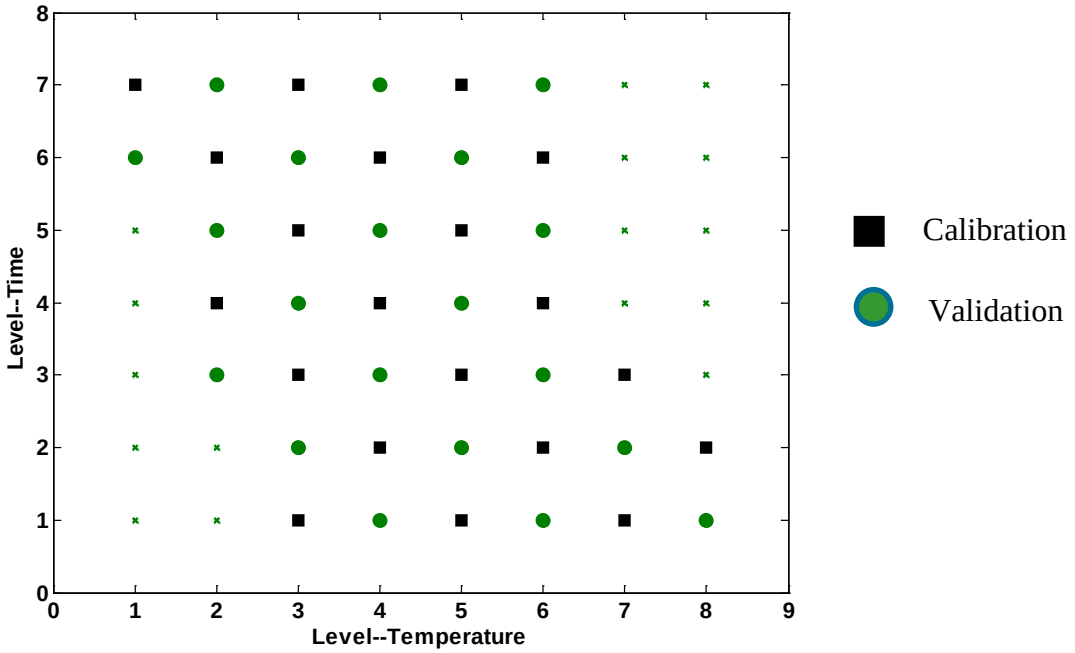

Figure 1. The DoE

Specific time and temperature exposure combinations (table 2) were used for the thermal damage investigations. Samples marked with an asterisk are the thermal exposure conditions for the 4″ coupons, which were used in the additional NDI investigations.

Table 2. Temperature and Time Exposures for Composite Thermal Damage Studies Based on DoE

Calibration Set			Evaluation Set		
Sample #	Temperature (°F)	Time (minutes)	Sample #	Temperature (°F)	Time (minutes)
1	385	30.00	1	415	30.00
2	445	30.00	2	475	30.00
3	505	30.00	3	535	30.00
4	415	48.11	4	385	48.11
5	475	48.11	5	445	48.11
6	535	48.11	6	505	48.11
7	385	77.14	7	355	77.14
8	445	77.14	8*	415	77.14
9	505	77.14	9	475	77.14
10	355	123.69	10	385	123.69
11	415	123.69	11	445	123.69
12	475	123.69	12	355	198.34
13*	385	198.34	13	415	198.34
14	445	198.34	14	475	198.34
15	355	318.05	15	325	318.05
16	415	318.05	16	385	318.05
17	475	318.05	17*	445	318.05
18	325	510.00	18	355	510.00
19	385	510.00	19*	415	510.00
20*	445	510.00	20	475	510.00

2.4 HEAT EXPOSURE PROCESS.

The thermal exposure of the test coupons was conducted at the University of Delaware CCM. The following process was followed to ensure the reliable exposure of the composite to the temperature and time variables:

- Reception of samples:
  - ~350 machined prepreg composite coupons were received from Boeing.
  - Coupons were sized for SBS tests (thickness = 0.1875″, width = 0.375″, length = 1.125″)

– Coupons were dried at a constant temperature of 125°F in a convection oven (figure 2) for 24 hours (coupon weight was monitored; no continuing weight loss was observed after 12 hours).

Figure 2. Received Composite Coupons in Drying Pan

- Thermal exposure process:

  – Coupons were exposed to heat in a medium-sized convection oven (Lindberg/Blue M MO1450A) for even temperature distribution.

  – The temperature was monitored with four NIST-certified J-type thermocouples (TCs) (OMEGA Eng. 5SC-GG-J-30-36) and a National Instruments 9211A USB-TC module (figure 3) using LabView Express software.

Figure 3. Temperature-Monitoring Setup

– The temperature measurements were acquired in various locations inside the oven—under/above the coupons and on the steel profiles (figure 4).

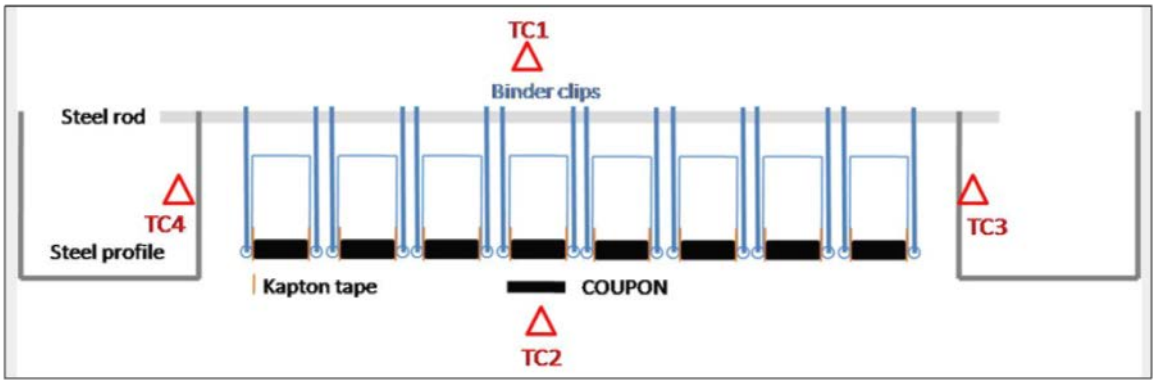

Figure 4. Schematic of Coupon Mounting and Thermocouple (TC) Locations

– The coupons were clamped by metal binder clips and protected by a layer of Kapton® tape to eliminate surface contact and interaction between coupon and clip (figure 5).

Figure 5. Coupon Clamped in Binder Clip

– The binder clips were hung from 12″ steel rods, situated upon steel U-profiles (figure 6).

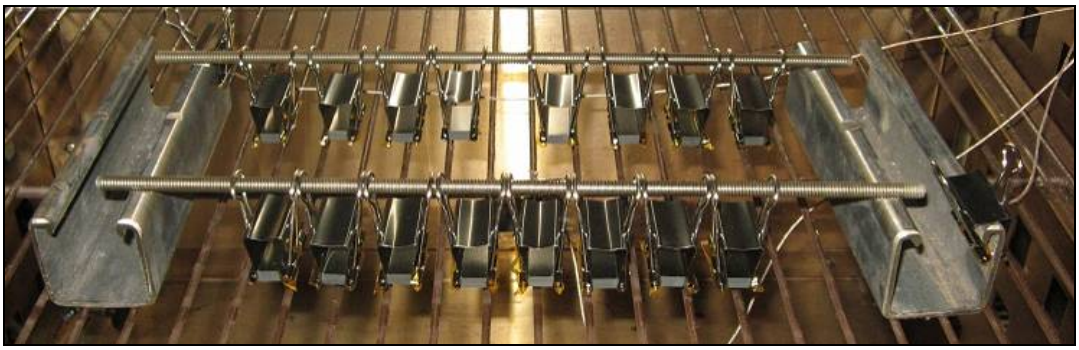

Figure 6. Clips Mounted on Steel Rod and Profiles

– After completion of the exposure time (table 3, figure 7), the oven was powered off and coupons were left inside to cool down slowly.

– This process was followed for both BMS8-256 and BMS8-276 coupons.

Table 3. Example Thermal Exposure Matrix for BMS8-256

Calibration Set			
Sample #	Temperature [°F]	Time [minutes]	Coupon Label
1	385	30	C1-1 to -6
2	445	30	C2-1 to -6
3	505	30	C3-1 to -6
4	415	48.11	C4-1 to -6
5	475	48.11	C5-1 to -6
6	535	48.11	C6-1 to -6
7	385	77.14	C7-1 to -6
8	445	77.14	C8-1 to -6
9	505	77.14	C9-1 to -6
10	355	123.7	C10-1 to -6
11	415	123.7	C11-1 to -6
12	475	123.69	C12-1 to -6
13	385	198.3	C13-1 to -6
14	445	198.34	C14-1 to -6
15	355	318.1	C15-1 to -6
17	475	318.05	C17-1 to -6
18	325	510	C18-1 to -6
19	385	510	C19-1 to -6
20	445	510	C20-1 to -6

Evaluation Set			
Sample #	Temperature [°F]	Time [minutes]	Coupon Label
1	415	30	E1-1 to -6
2	475	30	E2-1 to -6
3	535	30	E3-1 to -6
4	385	48.11	E4-1 to -6
5	445	48.11	E5-1 to -6
6	505	48.11	E6-1 to -6
7	355	77.14	E7-1 to -6
9	475	77.14	E9-1 to -6
11	445	123.69	E11-1 to -6
8	415	77.14	E8-1 to -6
10	385	123.7	E10-1 to -6
14	475	198.34	E14-1 to -6
12	355	198.3	E12-1 to -6
15	325	318.05	E15-1 to -6
13	415	198.3	E13-1 to -6
17	445	318.05	E17-1 to -6
18	355	510	E18-1 to -6
19	415	510	E19-1 to -6
20	475	510	E20-1 to -6

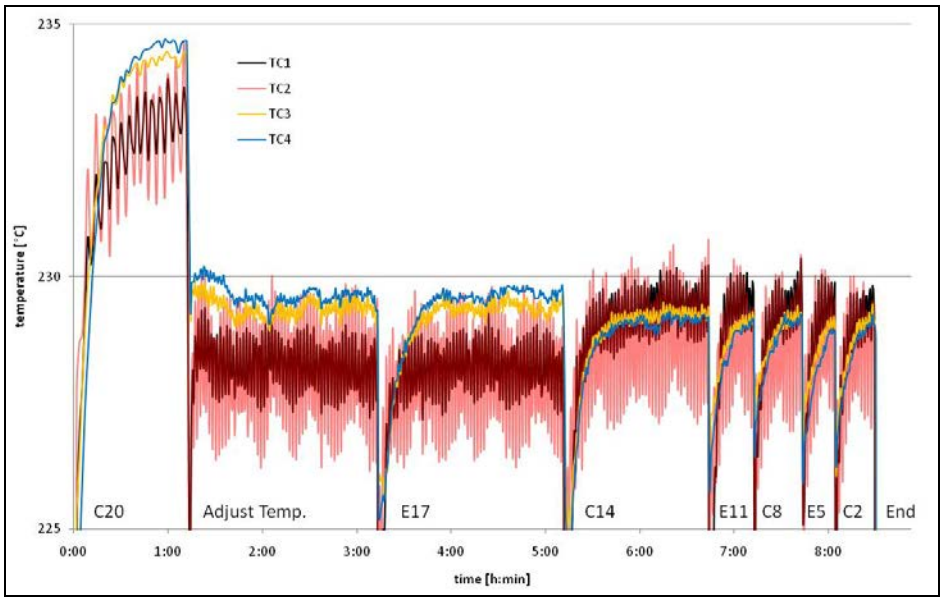

Figure 7. Example of Temperature History During Thermal Exposure of Composite Coupons Suspended in Oven

2.5 FTIR MEASUREMENTS.

All measurements were carried out using a 4100 ExoScan (figure 8) handheld FTIR analyzer (Agilent Technologies, formerly A2 Technologies, Danbury CT). Data were recorded at both 4 cm^{-1} and 8 cm^{-1} resolution; 75 and 120 interferograms, respectively, were co-added to produce the IR spectra. The spectra were recorded in the fingerprint region (i.e., from 1800 cm^{-1} to 650 cm^{-1}) using both 45-degree external reflectance and diffuse reflectance sampling interfaces. Composites were analyzed by FTIR in both the resin-rich region (surface of the composite coupon) and the resin-poor region (approximately 8 mm of the surface was removed via milling to reveal the fiber-rich region).

Figure 8. Agilent Technologies 4100 ExoScan System Mounted in Docking Station for Measurement of Thermal Damage in Composite Coupons (docking station enables analyzer to be used in lab for methods development)

The procedure for examining a particular time/temperature sample set via FTIR was as follows:

1. The background was collected using the gold diffuse reflectance reference cap.

2. Coupons were placed on the ExoScan with the center of the coupon over the sampling window.

3. The coupon was oriented for maximum energy as measured by the centerburst intensity of the raw interferogram.

4. The spectrum was collected at the desired acquisition parameters.

5. The left end of the coupon was moved over the sampling window, maintaining the optimum orientation.

6. The spectrum was collected at the desired acquisition parameters.

7. The right end of the coupon was moved over the sampling window, maintaining the optimum orientation.

8. The spectrum was collected at the desired acquisition parameters.

9. Steps 2 through 8 were repeated for the second and third replicate coupons.

The entire set of 4 cm^{-1} resolution measurements were made first, followed by the entire set of 8 cm^{-1} resolution measurements. The order of samples (depicted in table 4) was randomized using the Matlab® function randperm, which provides random permutations of a set of integers, in this case 1 to 40. This process was followed for both BMS8-276 and BMS8-256 coupons.

Table 4. Order for FTIR Measurements of BMS8-276 Composite Coupons

Measurement Order	4 cm^{-1}, 75 scans	8 cm^{-1}, 120 scans
1	C3	E12
2	E18	E20
3	C9	E2
4	E15	E14
5	E4	E15
6	C1	C6
7	E3	C3
8	C12	C16
9	E10	C11
10	C6	E10
11	C19	E13
12	E5	C7
13	C17	E18
14	E16	E8
15	E13	C17
16	C7	C14
17	C10	C8
18	C16	C5
19	E17	E9
20	E20	E1
21	C8	E5

Table 4. Order for FTIR Measurements of BMS8-276 Composite Coupons (Continued)

Measurement Order	4 cm^{-1}, 75 scans	8 cm^{-1}, 120 scans
22	C4	E17
23	E11	E11
24	E2	E7
25	C2	E6
26	E1	C19
27	C11	C15
28	E8	C1
29	E9	E16
30	E19	E3
31	C18	C2
32	C5	C4
33	E12	C18
34	C13	E4
35	C15	E19
36	E6	C13
37	E7	C9
38	C20	C20
39	C14	C10
40	E14	C12

C = Calibration, E = Evaluation

2.6 THE SBS MEASUREMENTS.

Measurements were carried out at the University of Delaware CCM using an Instron 4484 system (figure 9) equipped with an SBS fixture (figure 10). Exact coupon dimensions were recorded and the mechanical tests carried out according to the American Society for Testing and Materials (ASTM) D2344 standard procedure (table 5). The span length was 0.725 inches and a crosshead speed of 0.05 inches/minute was used.

Figure 9. The ASTM D2344 Setup on Instron 4484

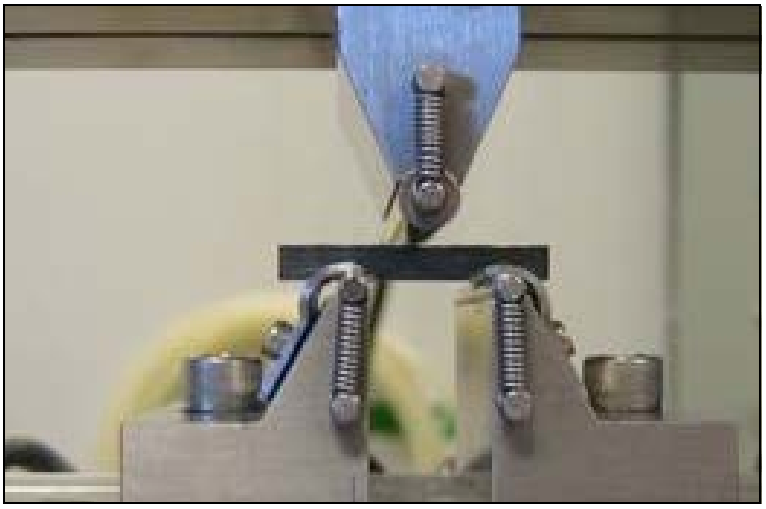

Figure 10. Detailed View of Coupon Mounting in Test Fixture

Table 5. Example of Coupon Dimensions for BMS8-276

Sample Group	Width [in.]	Thickness [in.]	Area [mm^2]	F^{sbs} [MPa]	StDev
C1	0.3593	0.1797	41.7	78.5	2.0
C2	0.3593	0.1800	41.7	76.4	3.9
C3	0.3588	0.1835	42.5	63.0	3.4
C4	0.3588	0.1803	41.7	76.3	2.9
C5	0.3583	0.1802	41.7	72.7	1.1
C6	0.3592	0.1835	42.5	43.0	1.0
C7	0.3588	0.1808	41.9	81.5	3.5
C8	0.3583	0.1792	41.4	75.1	4.1

Table 5. Example of Coupon Dimensions for BMS8-276 (Continued)

Sample Group	Width [in.]	Thickness [in.]	Area [mm^2]	F^{sbs} [MPa]	StDev
C9	0.3590	0.1795	41.6	54.0	3.8
C10	0.3565	0.1787	41.1	79.0	2.4
C11	0.3548	0.1792	41.0	77.6	1.6
C12	0.3573	0.1802	41.5	62.0	2.3
C13	0.3593	0.1802	41.8	81.4	3.8
C14	0.3617	0.1797	41.9	73.0	2.9
C15	0.3592	0.1810	41.9	80.2	2.9
C16	0.3528	0.1800	41.0	80.6	2.9
C17	0.3555	0.1788	41.0	55.6	3.8
C18	0.3605	0.181	42.1	86.5	5.8
C19	0.3593	0.1793	41.6	81.0	2.0
C20	0.3582	0.1792	41.4	74.2	2.7
E1	0.3595	0.1810	42.0	80.5	1.1
E2	0.3540	0.1775	40.5	76.2	1.9
E3	0.3583	0.1819	42.1	46.1	2.1
E4	0.3563	0.1788	41.1	80.5	5.0
E5	0.3538	0.1778	40.6	77.0	0.1
E6	0.3588	0.1822	42.2	54.4	1.2
E7	0.3585	0.1790	41.4	80.9	2.1
E8	0.3580	0.1798	41.5	80.4	3.2
E9	0.3522	0.1752	39.8	75.8	3.2
E10	0.3588	0.1793	41.5	78.4	1.6
E11	0.3587	0.1788	41.4	73.3	1.3
E12	0.3588	0.180	41.7	82.7	1.0
E13	0.3568	0.1788	41.2	76.2	1.8
E14	0.3562	0.1803	41.4	55.7	3.9
E15	0.3602	0.1802	41.9	91.0	1.0
E16	0.3593	0.1823	42.3	77.2	4.9
E17	0.3582	0.1802	41.6	75.4	1.9
E18	0.3532	0.1765	40.2	84.0	3.6
E19	0.3577	0.1782	41.1	76.0	1.3
E20	0.3567	0.1815	41.8	53.1	3.3

F^{sbs} = Short beam shear strength; StDev = Standard deviation

2.7 ULTRASONIC MEASUREMENTS.

Ultrasonic measurements were carried out on ten 4″ x 4″ coupons from each of the two different composites. After ultrasonic measurements were made on the unexposed coupons, they were exposed to the following temperature and time combinations (per DoE, table 1):

Calibration samples:

#13: 198.3 min at 385°F
#20: 510.0 min at 445°F

Evaluation samples:

#8: 77.14 min at 415°F
#17: 318.1 min at 445°F
#19: 510.0 min at 415°F

The panels were scanned tool-side up using a focused 10 Mhz transducer from Panametrics. The amplifier was set to 31.7 dB and a 5-20 Mhz filter was selected. Resolution was 1mm x 1mm and the scan area was 600 mm x 140 mm**.** Gate settings (offset by front surface reflection) were:

- Gate 02: 3.15µs, 0.18µs
- Gate 03: 3.30µs, 0.18µs
- Gate 04: 3.42µs, 0.18µs
- Gate 05: 3.117µs, 0.35µs

3. RESULTS AND DISCUSSION.

3.1 MECHANICAL TESTS.

The average SBS strengths of the thermally exposed BMS8-276 and BMS8-256 coupons are shown in tables 6 and 7, respectively, and graphically in figures 11 and 12, respectively.

Table 6. Average Absolute and Relative SBS Strength of BMS8-276

Sample Group	F^{sbs} [MPa]	StDev	Relative F^{sbs} [%]		Sample Group	F^{sbs} [MPa]	StDev	Relative F^{sbs} [%]
C1	84.4	1.4	95.1		E1	79.4	1.6	89.6
C2	76.5	2.9	86.2		E2	75.5	0.6	85.1
C3	72.0	3.6	81.1		E3	47.7	1.4	53.7
C4	80.7	3.3	90.9		E4	81.6	1.1	92.0
C5	74.5	0.9	84.0		E5	75.3	0.7	84.9
C6	43.9	0.9	49.5		E6	50.6	2.5	57.0
C7	83.0	1.6	93.5		E7	82.5	2.1	93.0
C8	76.0	3.2	85.6		E8	76.0	1.4	85.7
C9	52.0	0.8	58.6		E9	70.7	2.4	79.7
C10	82.1	2.5	92.5		E10	82.0	2.1	92.5
C11	79.3	1.7	89.4		E11	75.0	1.7	84.6
C12	61.8	3.1	69.7		E12	82.8	0.6	93.3
C13	81.9	2.6	92.3		E13	75.9	2.4	85.6
C14	73.5	1.4	82.9		E14	57.9	0.6	65.2
C15	82.8	2.9	93.3		E15	82.8	0.6	93.4
C16	79.1	0.7	89.2		E16	78.8	1.2	88.9
C17	55.9	1.6	63.0		E17	73.0	4.0	82.3
C18	83.5	3.8	94.2		E18	82.4	0.6	92.9
C19	76.2	5.4	85.9		E19	77.0	3.1	86.8
C20	72.8	1.1	82.0		E20	55.2	2.7	62.3

F^{sbs} = Short beam shear strength; StDev = Standard deviation

Table 7. Average Absolute and Relative SBS Strength of BMS8-256

Sample Group	F^{sbs} [MPa]	StDev	Relative F^{sbs} [%]		Sample Group	F^{sbs} [MPa]	StDev	Relative F^{sbs} [%]
C1	73.5	8.1	94.2		E1	78.8	2.0	101.0
C2	76.7	1.5	98.3		E2	46.9	0.9	60.2
C3	42.0	0.9	53.9		E3	35.7	0.5	45.7
C4	80.2	1.5	102.8		E4	78.0	1.6	100.0
C5	50.5	2.6	64.8		E5	72.0	7.7	92.3
C6	36.0	0.9	46.2		E6	39.4	1.1	50.5
C7	76.6	1.4	98.1		E7	75.8	6.9	97.2
C8	55.4	0.8	71.0		E8	79.2	1.1	101.6
C9	40.0	3.5	51.2		E9	47.3	0.7	60.7
C10	78.0	5.5	100.0		E10	78.9	1.9	101.1
C11	74.0	4.2	94.8		E11	54.3	1.9	69.6
C12	46.5	4.3	59.6		E12	78.2	1.6	100.2
C13	77.6	0.5	99.5		E13	73.5	6.0	94.2
C14	73.0	2.9	93.6		E14	46.6	3.6	59.7
C15	77.8	1.1	99.7		E15	78.6	2.2	100.8
C16	72.1	4.8	92.4		E16	79.3	2.3	101.7
C17	55.6	3.8	71.3		E17	50.6	3.0	64.9
C18	78.1	1.3	100.1		E18	77.6	1.9	99.5
C19	76.2	2.1	97.7		E19	67.2	6.7	86.1
C20	74.2	2.7	95.1		E20	47.8	0.6	61.3

F^{sbs} = Short beam shear strength; StDev = Standard deviation

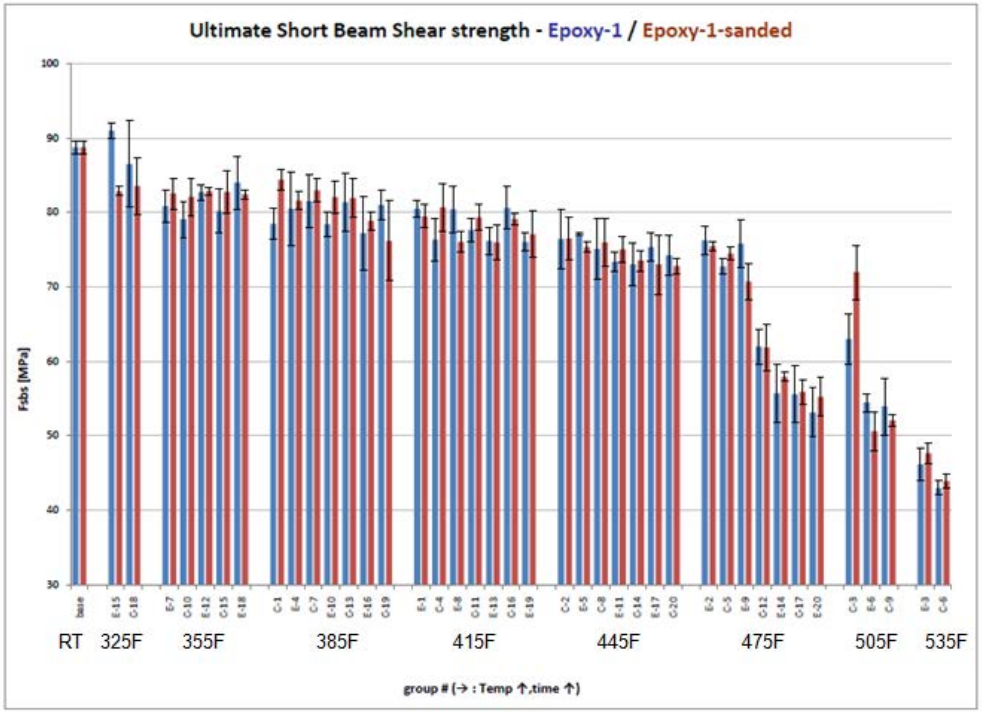

Figure 11. The SBS Strength for Both Sets of BMS8-276 Coupons

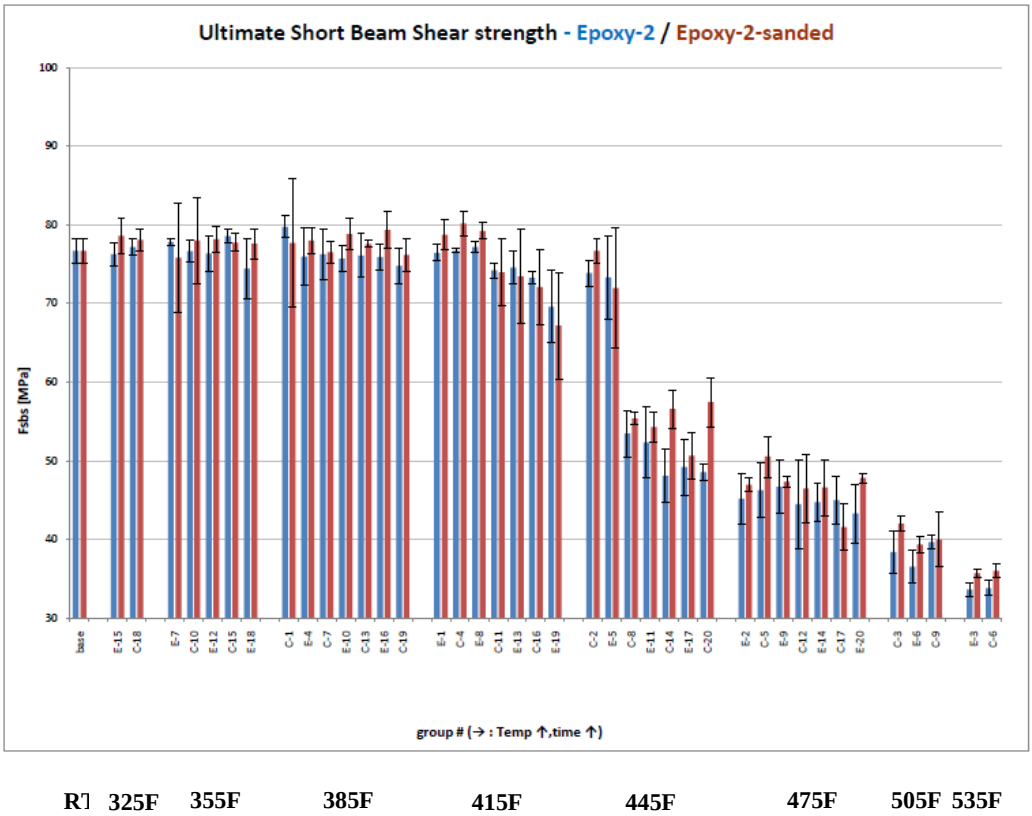

Figure 12. The SBS Strength for Both Sets of BMS8-256 Coupons

It is clear that there is little or no effect resulting from temperature on the mechanical strength of the coupons until the temperature reaches approximately 415°F. A fairly sharp transition occurs as the temperature approaches 475°F at longer thermal exposure and there is substantial damage above that point.

3.2 THE IR SPECTRA OF HEAT-TREATED COMPOSITE.

The IR spectra of the carbon fiber matrix composites are largely dominated by contributions from the epoxy resin. The carbon fiber does not contribute to the IR spectrum other than adding a scattering component. The shiny exterior surface of the composite coupons used in this study yielded excellent spectra when a specular reflection sampling interface was used in conjunction with the ExoScan FTIR analyzer.

When the composite coupons were exposed to heat at temperatures less than 400°F, the IR spectra demonstrated little or no change from untreated coupons, regardless of time of exposure. For exposures above 500°F, the IR spectra demonstrated significant change, indicative of oxidation of the composite. This is evidenced by the presence of a strong carbonyl band centered at 1720 cm^{-1}, as well as other changes in the polymer backbone region of the spectra (figure 13). The length of time of the exposure at temperature also has a significant effect on the degree of change that is observed in the IR spectra.

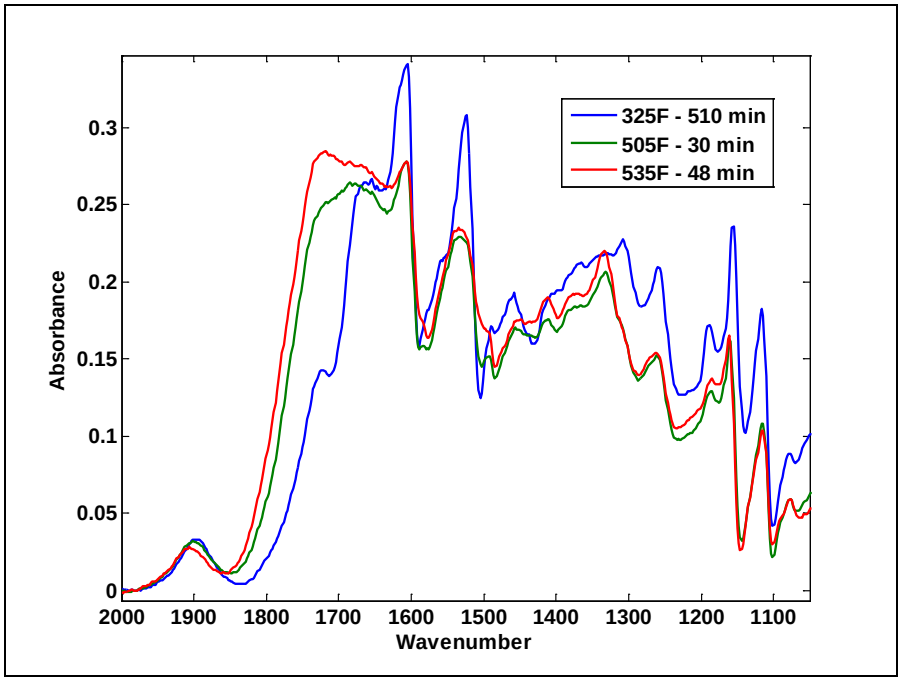

Figure 13. Specular Reflectance IR Spectra of Composite as a Function of Temperature and Time Exposure

These temperature ranges are related to actual situations to which the composite may be exposed. During either the manufacture of composite components or repair of composite aircraft, overheating of the material from heat lamps, thermal blankets, and other factors may occur.

Aircraft that are in service may experience localized overheating of composite components as a result of lightning strikes or exposure to jet engine heat. The presence of metal fasteners can also serve to focus heat and amplify the effect of localized heating.

3.3 DEPENDENCE OF SPECTRA CARBON FIBER/RESIN RATIO.

The overall goal of this project was to assess the value of a handheld FTIR spectrometer as a rapid, nondestructive, field-ready device for determining thermal damage in aircraft composites and enable the use of this technology as an aide in repairing damaged composites. Visible damage due to heat may not reflect the extent of underlying damage, nor is the damage from heat likely to be uniform. For this reason, an objective analysis of the degree and location of heat damage is important.

One common method of repairing composites is to sand-damage a section and then use a scarfed patch method to repair the sanded area. What needs to be determined is how much composite should be removed to ensure that pristine composite remains. Because the IR spectra of the composite is an indicator of molecular changes occurring as a function of thermal stress, a handheld IR spectrometer could be used as an objective guide for the technician to clearly identify the area that needs to be repaired and determine the extent and depth of the composite that needs to be removed.

The outer surface of the composite used in this study is largely composed of reflective epoxy resin. Both the specular reflectance and diffuse reflectance sampling interfaces for the handheld ExoScan FTIR provide spectra of similar quality (figure 14).

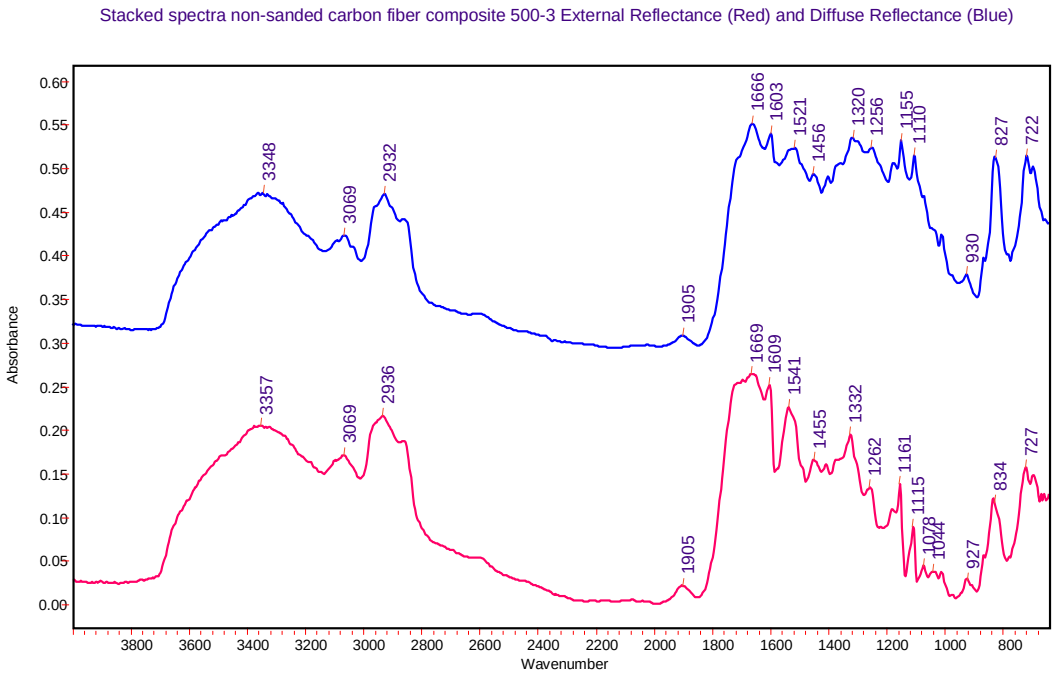

Figure 14. The IR Spectra of the Outer Surface of the Composite Coupon via Specular and Diffuse Reflectance

However, when the surface was sanded, the interior revealed a far higher ratio of carbon fiber to epoxy resin than at the surface. For this study, approximately 2 mm of the composite surface was removed via milling to reveal the interior.

In contrast to the resin-rich, fiber-poor exterior surface of the composite, which is quite reflective, the carbon fiber-rich interior of the coupons scatters IR radiation. A comparison of the specular and diffuse reflectance sampling methods shows that the latter technique provides higher quality spectra of the composite interior (figure 15). In both cases, the baseline shifts because of scattering by the increased amount of carbon fiber in the subsurface. However, the absorbance-to-noise ratio for the diffusely scattered light spectrum is 2 to 3 times higher than that of the external reflectance sampling interface. Specular reflectance of the interior surface still shows the presence of the polymer resin, but the amplitude of the vibration bands are attenuated relative to the information generated by diffuse reflectance.

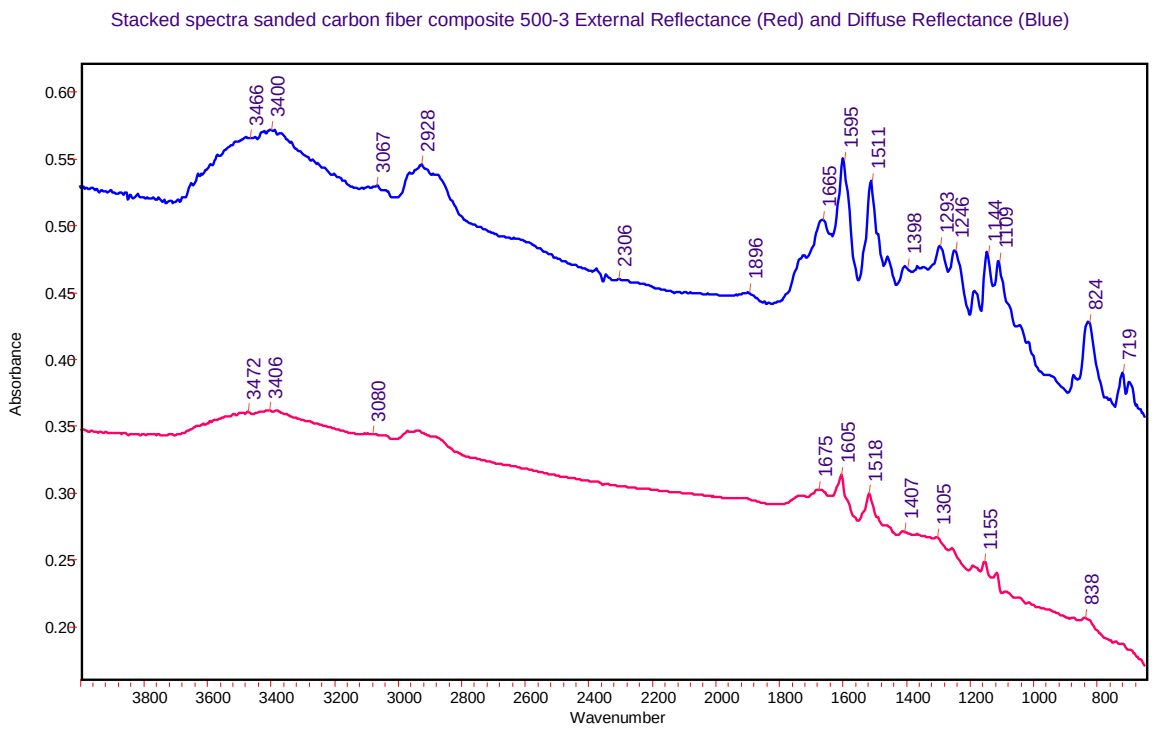

Figure 15. Comparison of Specular and Diffuse Reflectance IR Spectra for Sanded Composite (fiber-rich, resin-poor bulk region)

Overall, the general effect of localized overheating on the composite exterior surface can be readily detected by either specular or diffuse reflectance. Specular reflectance provides somewhat better quality spectra of the reflective composite exterior, whereas the diffuse reflectance sampling interface, which is designed to block the specular component of the reflected light, yields significantly better quality spectra for the fiber-rich interior of the composite.

3.4 RELATIONSHIP BETWEEN CHANGES IN SPECTRA AND MECHANICAL STRENGTH OF COMPOSITE.

A central goal of this project was to determine the relationship between the thermally induced chemical changes indicated by FTIR spectroscopy and the overall strength of the composite.

Specifically this research sought to:

1. Determine if the surface IR measurements can indicate bulk strength changes.

2. Develop calibrated methods for determining degree of thermal damage based on IR spectroscopy.

Whereas the SBS measurement is an indicator of overall bulk strength of the composite specimen, mid IR FTIR diffuse or specular reflectance measurements probe less than 10 microns of the coupon surface. The question arises whether a chemical change of the surface, as indicated by FTIR, can be an indicator of diminished composite sample strength. This is tested by determining if a mathematical correlation can be established between the FTIR data and the SBS measurements. Two approaches were undertaken to investigate the potential relationship between the two disparate measurement techniques. The FTIR and SBS data were correlated quantitatively using partial least squares (PLS), a classical multivariate correlation methodology. Also, FTIR data were analyzed via a neural net approach to determine if a method for classification of damage level could be developed that is totally independent of the SBS data.

3.5 THE PLS CORRELATION OF FTIR SPECTRA AND SBS DATA.

To determine the mathematical correlation between IR spectra and mechanical strength measurements, a calibration set was developed via a PLS method. The calibration set consisted of 20 coupons covering the temperature and time levels shown in table 2.

Triplicate measurements in three separate locations on each coupon surface resulted in 180 calibration spectra, each consisting of 120 co-added interferograms recorded at 8 cm^{-1} resolution. The spectra were analyzed in the 2013 cm^{-1} to 1187 cm^{-1} region and preprocessed to remove baseline effects via a second derivative using a 7-point Savitsky Golay smoothing algorithm. These spectra were correlated via the PLS method with the SBS strength measurements. Calibrations were then developed for the two different epoxy composites. Generally, a good fit was obtained for the data, and the quality of the calibration was determined by calculating the standard error, percent error, and correlation function, R^2. A cross validation analysis was carried out to initially evaluate the calibrations.

To determine how well these calibrations would predict physical strength of heat-damaged composite samples, a set of 20 evaluation samples—which were exposed according to the protocol detailed in table 2—were analyzed by FTIR and the results evaluated via the calibration. The data for these predicted sets (tables 8 and 9) demonstrate that the PLS method provides good correlation between the IR spectra and the mechanical strength measurements.

When correlating the FTIR data with the SBS data, it must be considered that the referee SBS method has inherent measurement error and, thus, the performance of the calibration can only be as good as the degree of error in the referee technique. In general, the SBS and FTIR data correlation was acceptable, taking into account the inherent error in both methods. Outlier analysis carried out on this data reflected improved data quality with respect to percentage error and R^2 function.

Table 8. Results of Spectra/Mechanical Strength Correlation for BMS8-276 Evaluation Set

Composite 1 – Tool Side – Specular Reflectance – 8 cm^{-1}/120 Scans			
	RMS Error	% Error	R^2
Calibration	1.48	1.6	0.98
Cross Validation	2.86	3.5	0.94
Prediction—Set 1	2.70	3.2	0.94
Prediction—Set 2	3.64	4.3	0.90

RMS = Root mean square

Table 9. Results of Spectra/Mechanical Strength Correlation for BMS8-256 Evaluation Set

Composite 2 – Tool Side – Specular Reflectance – 8 cm^{-1}/120 Scans			
	RMS Error	% Error	R^2
Calibration	3.08	4.3	0.96
Cross Validation	4.44	6.4	0.92
Prediction—Set 1	4.54	5.9	0.93

RMS = Root mean square

These calibrations and predicted values result from the IR specular reflectance measurement of the resin-rich, unsanded composite coupons. In contrast, we found that sanded composite was not as effectively analyzed by specular reflectance. The comparison of the FTIR correlations with mechanical strength (tables 10 and 11) clearly shows the difference in the statistical data acquired for sanded composite and unsanded material. When specular reflectance IR

spectroscopy is used for measuring sanded material, the RMS error, percentage error, and R^2 values are all negatively impacted relative to those of the unsanded composite.

Table 10. Results of Spectra/Mechanical Strength Correlation for Sanded BMS8-256 Evaluation Set

Composite 2 – Sanded – Specular Reflectance – 8 cm^{-1}/120 Scans			
	RMS Error	% Error	R^2
Calibration	6.69	9.6	0.82
Cross Validation	7.66	10.1	0.76
Prediction—Set 1	6.87	11.4	0.82

RMS = Root mean square

Table 11. Results of Spectra/Mechanical Strength Correlation for Unsanded BMS8-256 Evaluation Set as Measured by Specular Reflectance

Composite 2 – Unsanded – Specular Reflectance – 8 cm^{-1}/120 Scans			
	RMS Error	% Error	R^2
Calibration	3.08	4.3	0.96
Cross Validation	4.44	6.4	0.92
Prediction—Set 1	4.54	5.9	0.93

RMS = Root mean square

As a result of the requirement to measure sanded composite, a new diffuse reflectance sampling interface was developed for the 4100 ExoScan system. Diffuse reflectance is a preferred technique when a sample absorbs and/or scatters IR radiation, such as in the case of sanded composite.

When the sanded composite samples were evaluated by the diffuse reflectance sampling method, the quantitative results (table 12) were in line with those obtained for the unsanded samples using the specular reflectance method, as reported in table 11.

Table 12. Results of Spectra/Mechanical Strength Correlation for Sanded BMS8-256 Evaluation Set as Measured by Diffuse Reflectance

Composite 2 – Sanded – Diffuse Reflectance – 8 cm^{-1}/120 Scans			
	RMS Error	% Error	R^2
Calibration	3.00	4.1	0.96
Cross Validation	4.91	7.3	0.91
Prediction—Set 1	5.11	7.4	0.90

RMS = Root mean square

3.6 NEURAL NET ANALYSIS OF FTIR DATA.

The purpose of the neural net analysis was to determine if a method could be developed that provides accurate classification of the degree of thermal damage based on FTIR data, independent of the SBS mechanical strength measurements.

To classify the data, a neural network was trained via the scaled conjugate method using the Neural Network Toolbox™ from MathWorks. All samples were divided into four damage classifications: none, low, medium, and high. The network contained 30 hidden layer neurons and four output neurons corresponding to each of the damage classifications (figure 16). When a spectrum was presented to the network, values were calculated for each of the four output neurons. The output neuron with the highest value determined the level of damage.

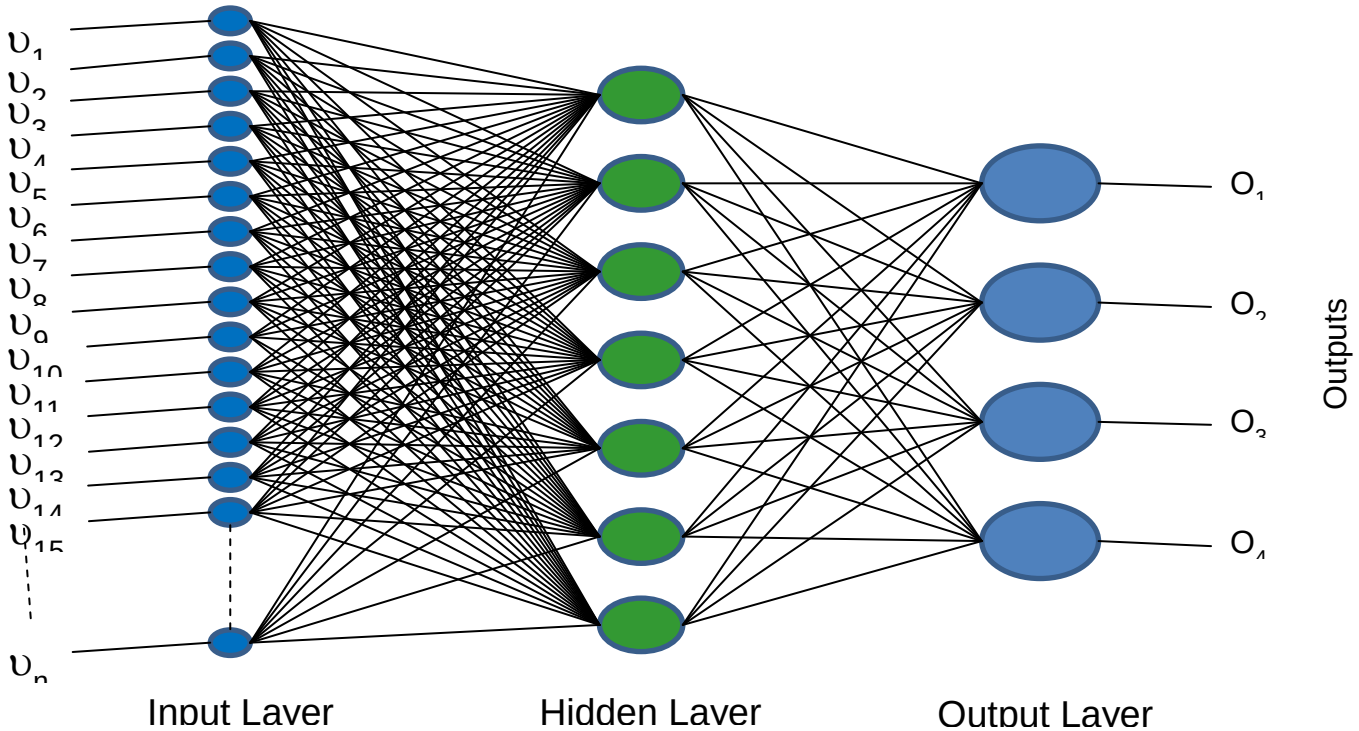

Figure 16. Neural Network Architecture Used for the Evaluation of Thermally Damaged Composite Coupons

Specular reflectance FTIR spectra of resin-rich BMS8-276 samples, which were presented to the network, consisted of 120 co-added interferograms recorded at 8 cm^{-1} resolution. The wavelength range was between 1954 cm^{-1} and 725 cm^{-1} and was pre-processed via a Savitzky-Golay second derivative (15 point, 2nd order). The resulting spectra were normalized to a unit area between 1454 cm^{-1} and 1197 cm^{-1}. Only the 1454 cm^{-1} to 1197 cm^{-1} segment was processed further. The network analyzed 180 training spectra and 180 independent spectra were then evaluated by the trained network.

The MATLAB Neural Network Toolbox output (figure 17) for summarizing predicted (output class) vs. actual (target class) results was generated by predicting damage levels of the independent set of evaluation samples (i.e., none of the samples were used to develop the neural network). All the outputs are shown for a given target class. Correct predictions are found in the green squares along the diagonal where predicted class equals actual class. Percentages within squares show the percentage of the total samples that have this target/output combination. Incorrect predictions are found off the diagonal. For example, two samples with high damage were predicted to have medium damage and two samples with no damage were predicted to have low damage. Percentages along the bottom are for the target (actual) classes (i.e., for a given target class, the percentage correctly predicted). Percentages along the side are for the output (predicted) classes (i.e., for a given output class, the percentage correctly predicted). The number shown in the bottom right (in blue) corresponds to the total percentage predicted correctly; thus, 97.8% of the unknown samples were classified correctly.

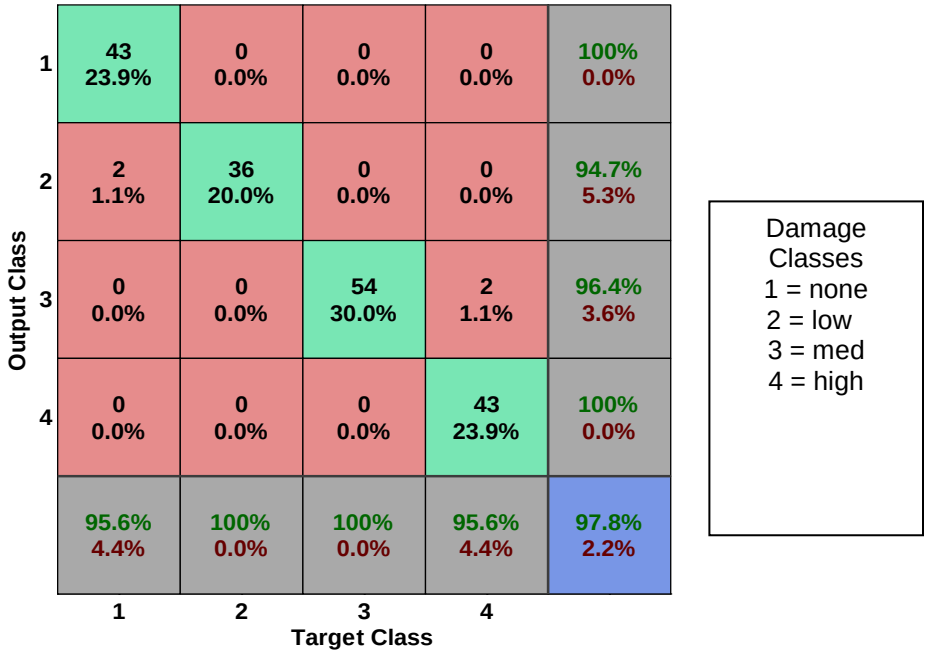

Figure 17. Neural Network Toolbox Output for Summarizing Predicted (output class) vs. Actual (target class) Results Based on FTIR Data Independent of SBS Results

This work has shown that carbon fiber epoxy resin composite samples that have been exposed to temperatures from 400°F to 525°F for various exposure times demonstrate different degrees of loss of strength associated with the conditions of exposure. Specular reflectance and diffuse reflectance FTIR spectra of these composite samples reflect changes indicative of degradation of the chemical bonds of the resin component of the composite matrix. Specular reflectance FTIR is most useful for measuring the shiny composite surface, which predominantly consists of the epoxy resin. Diffuse reflectance measurements are most effective for analyzing the sanded internal surface of the composite due to the high concentration of scattering carbon fiber. Using PLS multivariate analysis, the chemical information produced by the FTIR spectra and the mechanical strength formation provided by the SBS measurements can be correlated, supporting the hypothesis that FTIR surface analysis reflects the change in the bulk strength of the composite. A neural network approach proved to be effective for discriminating thermal damage FTIR measurements, independent of the SBS measurements.

3.7 USE OF EXOSCAN ANALYZER FOR MAPPING SURFACE OF DAMAGED COMPOSITE PANEL.

The correlation has been demonstrated between changes in mechanical strength and IR spectra as a function of temperature and time. If an aircraft is struck by lightning, localized heating could affect the composite and the extent of the damage is likely to be nonuniform. To simulate this event, a straightforward method for mapping positional damage across a larger composite surface was developed.

The process for carrying out this simulation is illustrated in figures 18-29.

12″ square panels were thermally stressed via a heat blanket with varied levels of insulation to obtain nonuniform damage. TCs monitored the heat at various locations (figure 18).

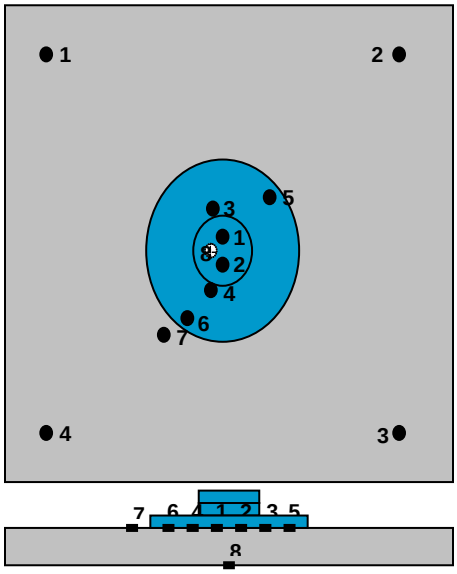

Figure 18. Thermocouple Location

The edges of the heat-damaged panels were lined with tape.

Figure 19. Composite Panel Lined With Tape

Simple grid markings were placed on the tape to facilitate the mapping experiment.

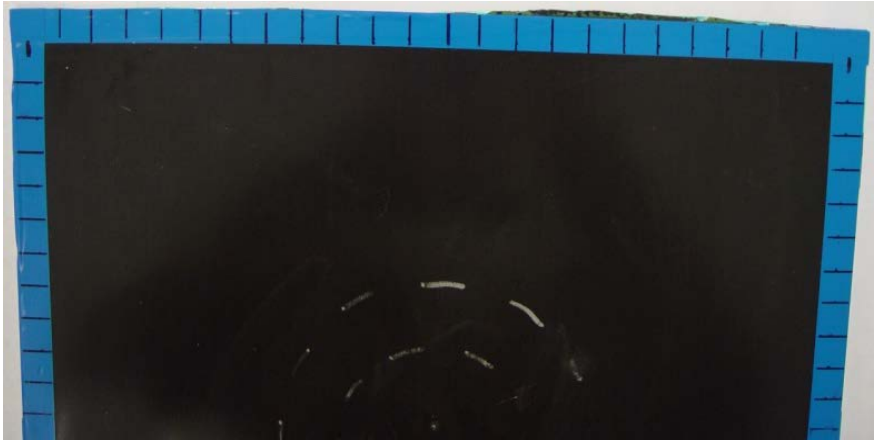

Figure 20. Setup and Markings on Tape

Transparencies were affixed to the panels to preserve TC locations once the silver markings on the panels are removed.

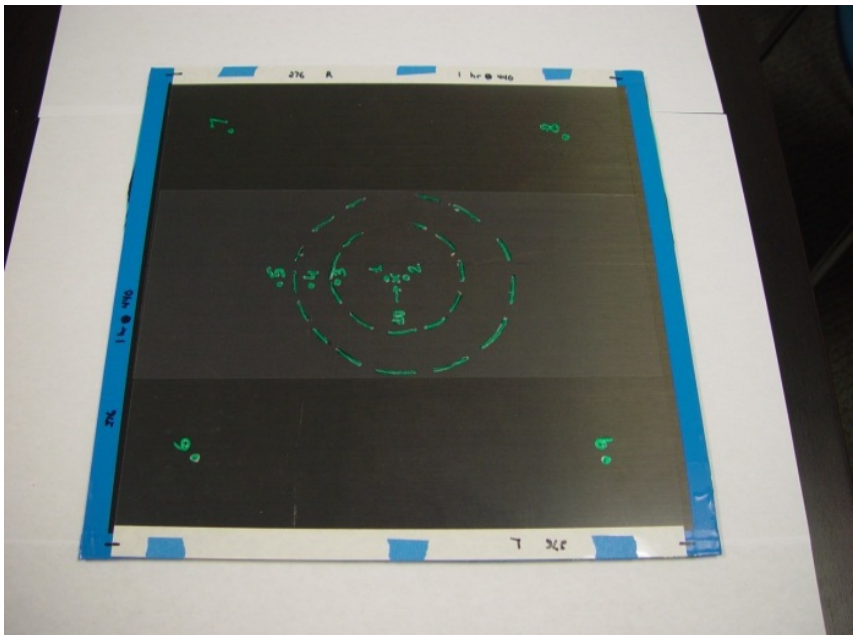

Figure 21. Composite Panel With Transparencies

Because these samples were heated in a vacuum, the resin-rich spectra of these panels do not match the resin-rich measurements of the earlier 1″ coupons. In separate experiments at Boeing, it was determined that scuffing the panels with a ScotchBrite™ pad would reveal a composite layer that produces spectra matching those collected on the 1″ coupons.

The ExoScan was fitted with a stand to facilitate repetitive measurements.

Figure 22. ExoScan Fitted With Stand

The proper orientation of the ExoScan was determined through examination of the real-time IR signal. Since fiber orientation is consistent throughout the panel, the same ExoScan orientation can be used for all measurements.

The sampling interface of the ExoScan was marked to facilitate realignment of the system while mapping the panel surface.

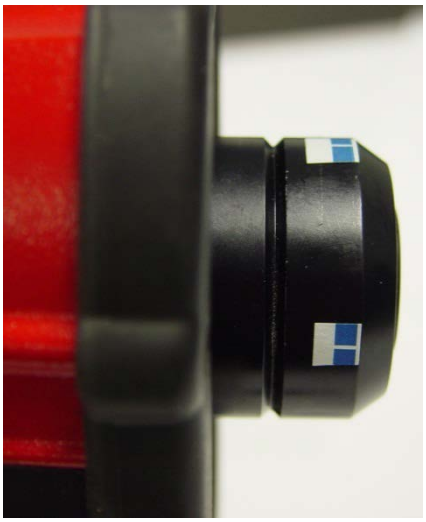

Figure 23. ExoScan Closeup

Laser levels were positioned along the grid to locate the ExoScan in the appropriate position for the mapping experiment.

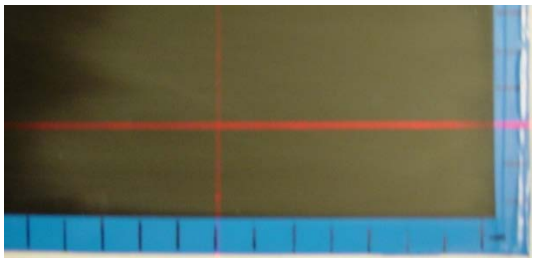

Figure 24. Laser Levels

The ExoScan was positioned using the laser lines in order to collect a spectrum.

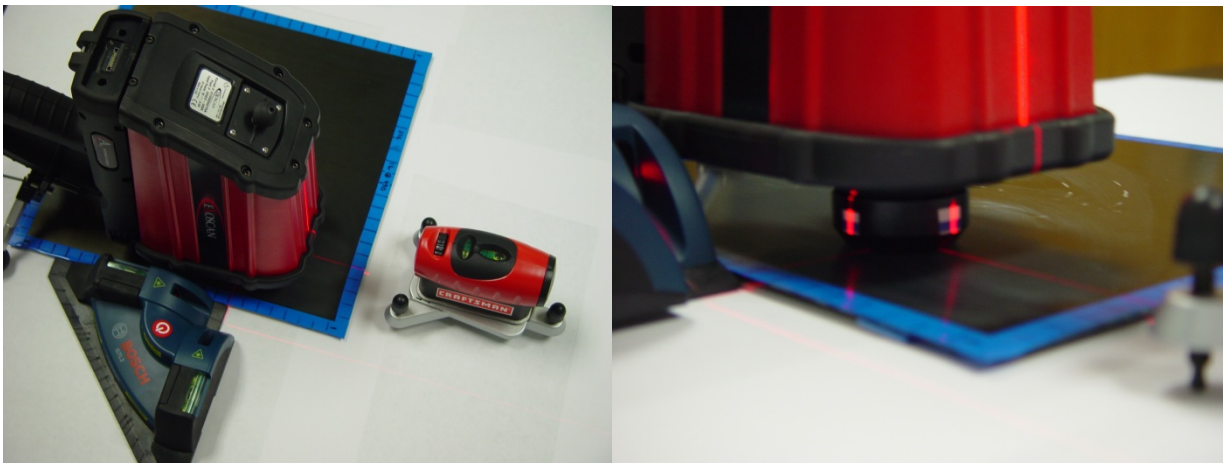

Figure 25. ExoScan Laser Positioning

Three 12″ x 12″ panels of BMS8-276 were exposed to maximum temperatures of 490°F, 465°F, and 440°F to produce thermal damage. By placing different layers of insulation between each panel and the heating elements, nonuniform temperatures were induced, producing nonuniform damage across the panel. Each panel was mapped with 361 separate FTIR measurements using the ExoScan equipped with a diffuse reflectance sampling interface.

The results of these mapping experiments are shown in the two-dimension (figure 26) and three-dimension contour plots (figure 27), which relate the increasing IR carbonyl band absorbance value, an indicator of oxidation (i.e., thermal damage) as a function of position on the large panel. These plots graphically illustrate the increasing damage as a function of temperature. All of the data in this last plot has been normalized—the areas of greatest heat damage are in red-brown; the areas of least damage are in dark blue. As expected, the intensity and degree of damage increases with thermal exposure, as indicated by the amount of red coloration in the map. The 490°F panel appears to exhibit some damage across much of the 12″ x 12″ panel.

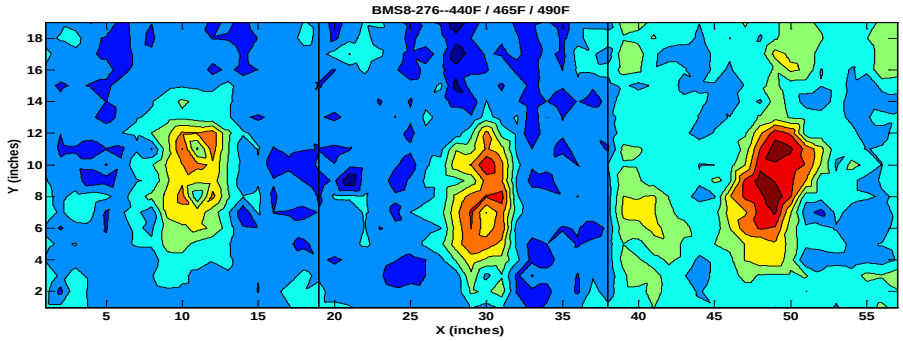

Figure 26. Contour Maps for Thermal Damage as a Function of Distance for Panels Exposed to Increasing Levels of Thermal Stress (blue indicates the least-damaged regions; brown indicates the most-damaged regions)

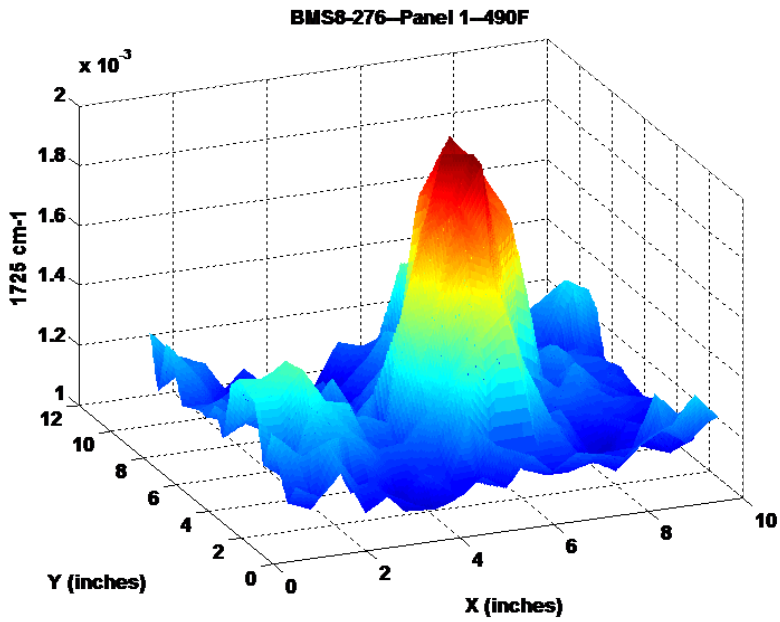

Figure 27. Thermal Damage as a Function of Position for Composite Panel Exposed to Highest Levels of Heat

This ability to define and map areas of greatest thermal damage over larger parts may be an aid to maintenance operations which are associated with scarf/patch repair of heat damaged composites. The IR results can show the operator where damaged composite is situated, delineate the edges of the damaged region, and reveal where undamaged composite begins. With coordinated sanding and measurement via the IR system, defining the breadth and depth of the patch required may be aided.

3.8 THERMAL DAMAGE – ADDITIONAL STUDIES IN THE "TRANSITION" RANGE.

There was significant interest in creating and analyzing samples of composite that fall into the damage transition range (i.e., that combination of temperature and time for which the composite begins to change from being acceptable, with respect to molecular structure, to showing signs of degradation due to thermal stress). The reason was to gather more comparison information about the abilities of different NDI methods to detect incipient thermal damage. Specifically, the larger coupons were needed for advanced NDI methods carried out at AANC.

Sixty three 4″ x 4″ coupons were prepared at Boeing, heat exposed at CCM, and then shipped to AANC for evaluation by a variety of NDI methods. These coupons were sized at 4″ x 4″ to enable classical NDI methods to be used; they were resized after NDI measurement for the SBS work. The FTIR measurements were carried out both at AANC and A2 Technologies. The SBS values were obtained at CCM.

3.9 BMS8-276 4″ COUPONS.

Coupons of BMS8-276 were exposed to a range of time and temperature combinations (table 13). Samples 1, 5, 9, 14, and 19 at 475°F are highlighted because they were inadvertently exposed to the temperature for too long.

Table 13. The SBS Data for 4″ BMS8-276 Coupons, Which Were Analyzed at AANC and Then Cut Into 1″ Size for SBS Analysis at CCM

Sample #	Temp (°F)	Time (min)	F^{sbs} [MPa]	Standard Deviation [MPa]	% of Baseline
2	490	30	44.0	1.8	57.4
3	505	30	12.0	1.1	15.7
4	460	50	49.3	1.5	64.2
6	490	50	17.1	2.9	22.3
7	505	50	10.3	1.3	13.4
8	460	70	47.6	2.3	62.1
10	490	70	16.8	1.6	21.9
11	505	70	11.2	1.5	14.6
12	445	90	50.0	1.4	65.2
13	460	90	46.4	0.8	60.5
15	490	90	14.4	3.1	18.8
16	505	90	11.2	1.8	14.6
17	445	120	48.0	0.9	62.6
18	460	120	43.6	1.3	56.8
20	490	120	11.6	1.6	15.2
21	505	120	10.9	1.6	14.3

Table 13. SBS Data for 4″ BMS8-276 Coupons, Which Were Analyzed at AANC and Then Cut Into 1″ Size for SBS Analysis at CCM (Continued)

Sample #	Temp (°F)	Time (min)	F^{sbs} [MPa]	Standard Deviation [MPa]	% of Baseline
1	475	70	39.2	0.9	51.1
5	475	90	30.2	1.4	39.3
9	475	110	18.3	2.6	23.8
14	475	130	16.7	2.6	21.8
19	475	160	16.2	1.4	21.2

F^{sbs} = Short beam shear strength

One observation is that the force required to shear these samples appeared different from that observed in the earlier 1″ coupon data. For example, the maximum F^{sbs} value of 50.0 and the percentage of baseline of 65.2% for the lowest time/temperature combination in the 4″ coupon set (445°F; 90 minutes) was approximately 70% of what was observed for those values in the earlier 1″ coupon data. It is unknown whether this was due to a calibration issue for the SBS equipment or if the equipment was somehow different from that used in the earlier work, but the overall result is that the SBS-FTIR PLS calibrations previously developed would not be useful to analyze this data set. What is interesting, however, is that although the SBS results are different, the plot of F^{sbs} versus time/temperature (figures 28 and 29) appears quite similar to that of the earlier work, with relative values demonstrating similar trends, and does cover the low/medium/high damage exposure combinations, as intended.

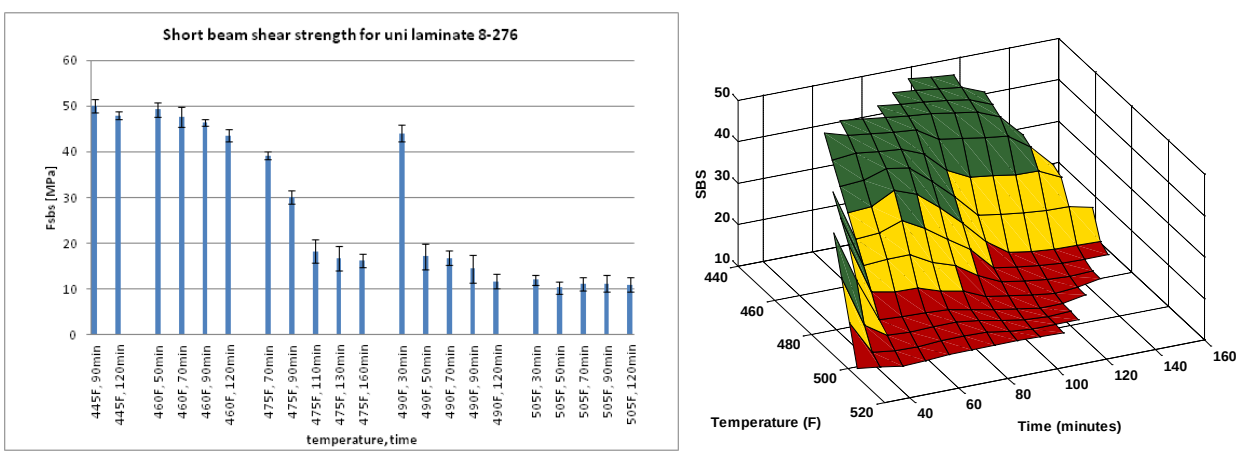

Figure 28. Force vs. Temperature/Time Combinations for BMS8-276 (4″ x 4″ coupons)

The IR data (figure 29) were obtained on these samples using the ExoScan system and conditions for processing the IR data were the same as used for the earlier 1″ coupons. The

frequency range used was 1985 cm^{-1}-1588 cm^{-1} and the spectra were preprocessed by baseline correcting at 1985 cm^{-1}. The range from 1985 cm^{-1}-1588 cm^{-1} was normalized to unit length.

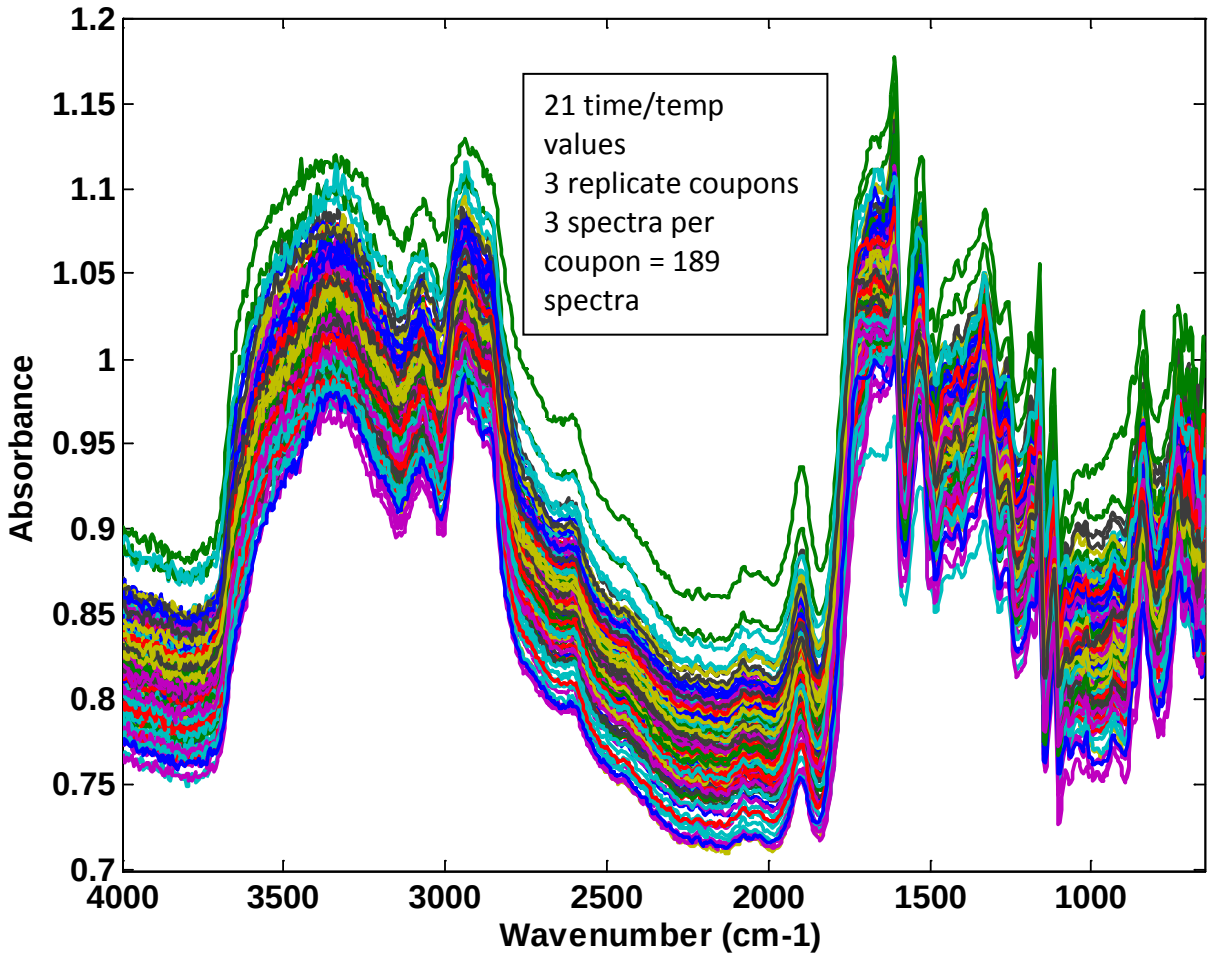

Figure 29. The IR Spectra for BMS8-276 (4″ coupons)

Cluster analysis of the FTIR data was carried out (figure 30) and the colors in figure 31 are consistent with colors of the spectral clusters (figure 32). The FTIR analysis demonstrates similar trends when compared to the SBS data and indicates that the 4″ coupon sample set does define a range of damage conditions.

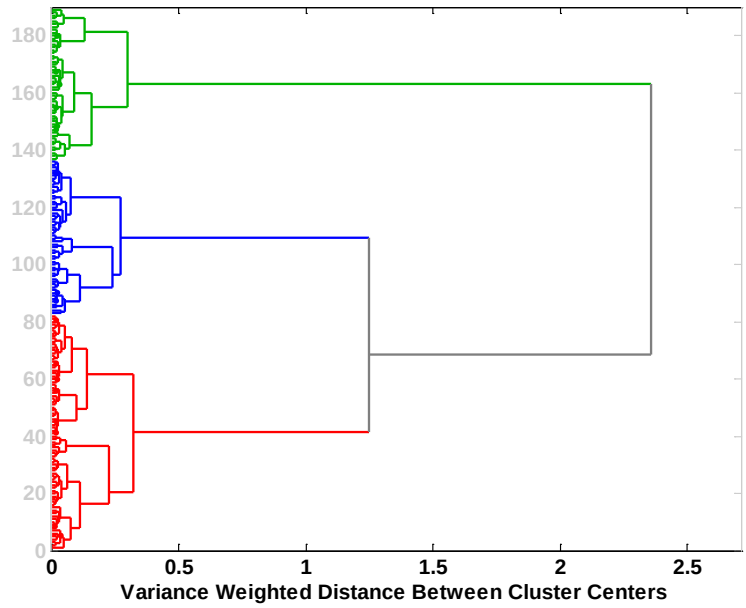

Figure 30. Cluster Analysis of Spectral Data for BMS8-276 (4″ coupons)

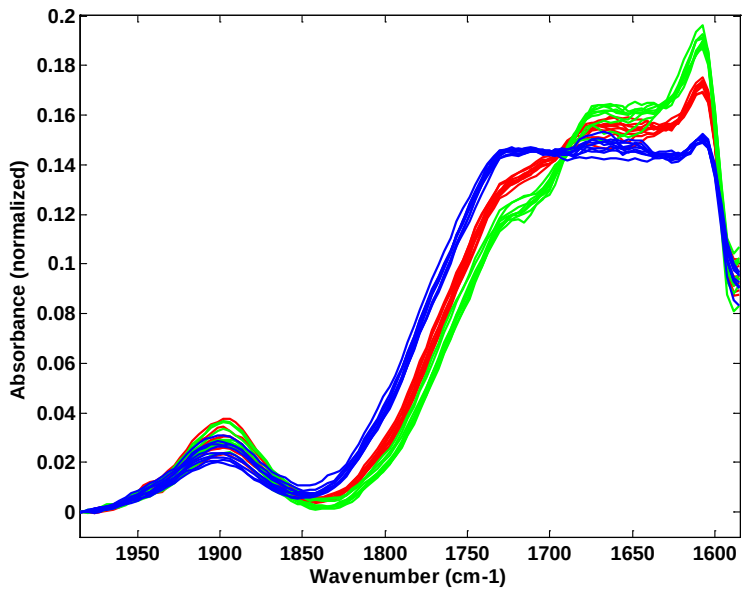

Figure 31. Spectra Clustering of Low, Medium, and High Damage Within the Dataset for 4″ BMS8-276 Coupons

Changes in the spectra (figure 32) for the 4″ coupons exposed to 490°F for increasing amounts of time are readily evidenced by the increasing carboxyl absorbance value. This combination of temperature at increasing exposure times is an example of the spectral changes that occur as the composite transitions from lower to higher levels of resin oxidation.

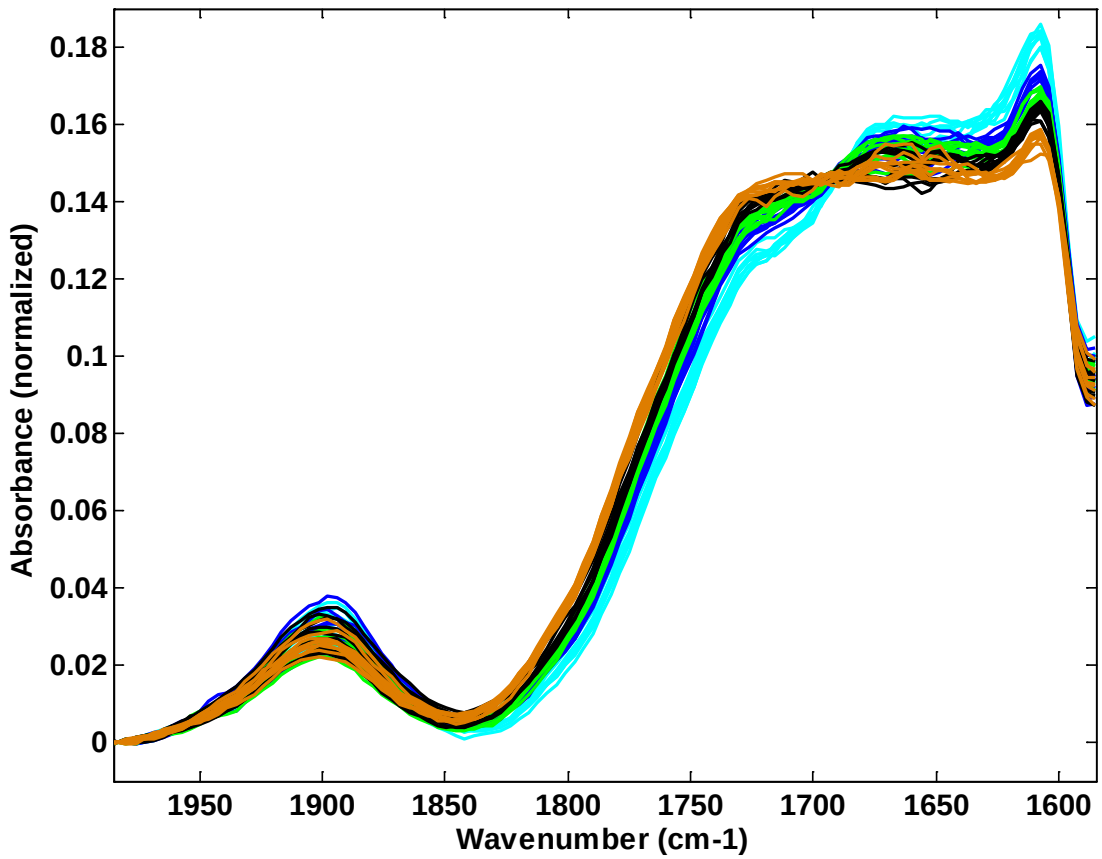

Figure 32. Spectra of Composite Exposed to 490°F for Progressive Times – 30 Minutes (cyan), 50 Minutes (blue), 70 Minutes (green), 90 Minutes (black), and 120 Minutes (orange)

When the spectra of the 490°F exposed 4″ coupons are overlaid with those of 1″ coupons that had experienced the minimum and maximum temperature/time exposures (figure 33), the IR spectral data appear quite consistent, even if the SBS data were not. The relative difference in spectral characteristics in the transition range, as compared to the spectra of coupons with maximum or minimum exposure, are consistent and support the value of the FTIR measurement for detecting incipient thermal damage.

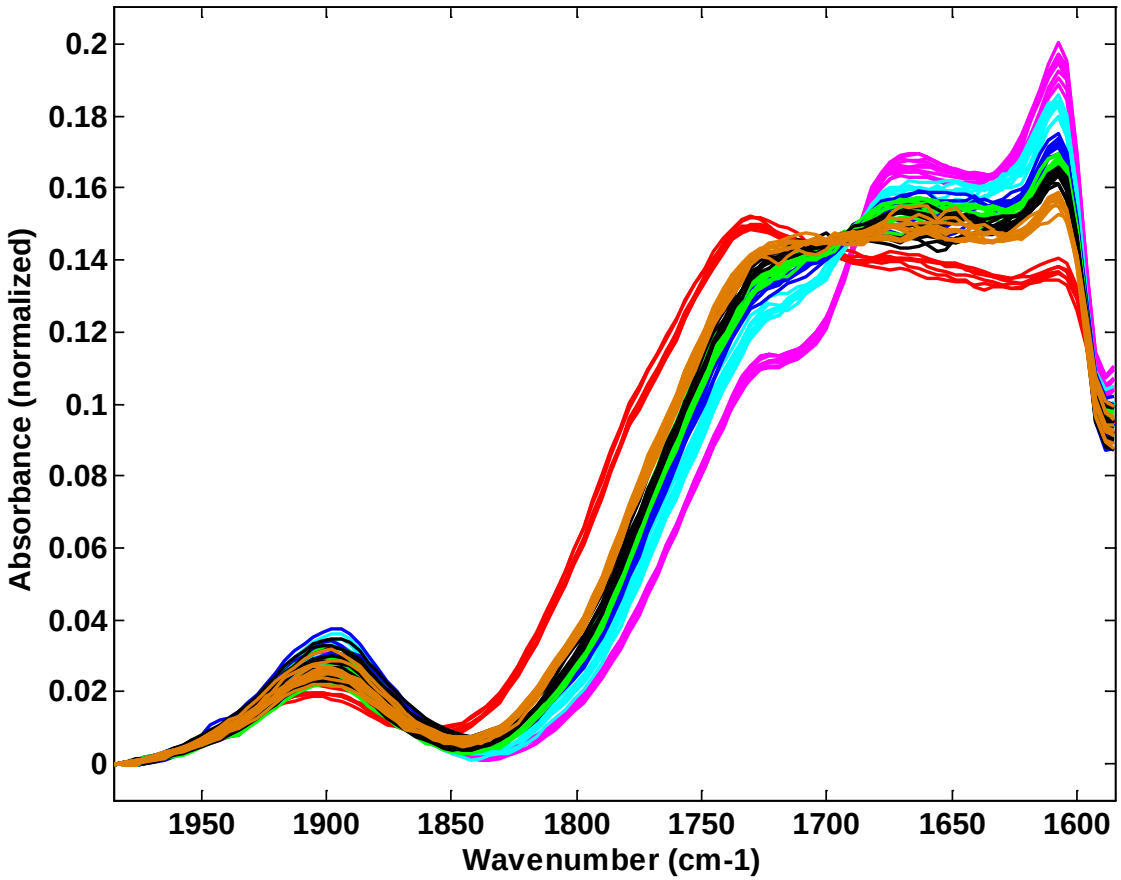

Figure 33. Spectra of 4″ BMS8-276 Coupons Exposed to 490°F for Progressive Times – 30 Minutes (cyan), 50 Minutes (blue), 70 Minutes (green), 90 Minutes (black), and 120 Minutes (orange) Overlayed With Minimum (purple) and Maximum (red) Thermally Exposed 1″ Coupons

3.10 BMS8-256 4″ COUPONS.

As discussed in section 3.9, coupons of BMS8-256 were exposed to a range of time and temperature combinations (see table 14).

Table 14. The SBS Data for BMS8-256 4″ Coupons, Which Were Analyzed at AANC and Subsequently Cut Into 1″ Size for SBS Analysis at CCM

Sample #	Temperature (°F)	Time (min)	F^{sbs} [MPa]	StDev. [MPa]	% of Baseline
1	445	30	72.4	4.1	81.6
2	460	30	72.3	0.3	81.5
3	475	30	28.1	4.1	31.7
4	430	50	72.9	1.7	82.1
5	445	50	72.0	1.1	81.2
6	460	50	31.3	4.4	35.3
7	475	50	32.5	3.9	36.7
8	430	70	73.5	1.7	82.8
9	445	70	37.0	5.5	41.7
10	460	70	34.8	1.9	39.2
11	475	70	26.5	5.6	29.9
12	415	90	71.3	1.6	80.4
13	430	90	71.2	0.7	80.3
14	445	90	37.3	5.9	42.0
15	460	90	32.0	4.8	36.1
16	475	90	33.8	3.7	38.1
17	415	120	74.2	0.9	83.6
18	430	120	75.3	1.2	84.9
19	445	120	37.8	5.5	42.6
20	460	120	31.9	6.1	36.0
21	475	120	27.0	3.6	30.4

F^{sbs} = Short beam shear strength; StDev. = Standard Deviation

As we observed for the BMS8-276 samples, the force required to shear these samples is different than that required for the earlier 1″ coupon measurements. For the 4″ BMS8-256 coupons, the maximum F^{sbs} value of 75.3 and the percentage of baseline of 84.9% for the low time/temperature combination is somewhat more consistent with that observed for the 1″ BMS-256 coupons (and not as greatly varying, as was observed for BMS8-276). It is unknown whether this is due to a calibration issue of the SBS equipment or if the equipment was somehow different from that used in the earlier work, but the overall result is that the SBS-FTIR PLS calibrations developed for the 1″ coupons BMS8-256 would not be useful to analyze the 4″ coupons.

As in the previous case, although the absolute SBS results are different, the plots of F^{sbs} versus time/temperature (figure 34) look quite similar to that of the earlier work and accurately demonstrate the progressive composite weakening in the transition temperature regime.

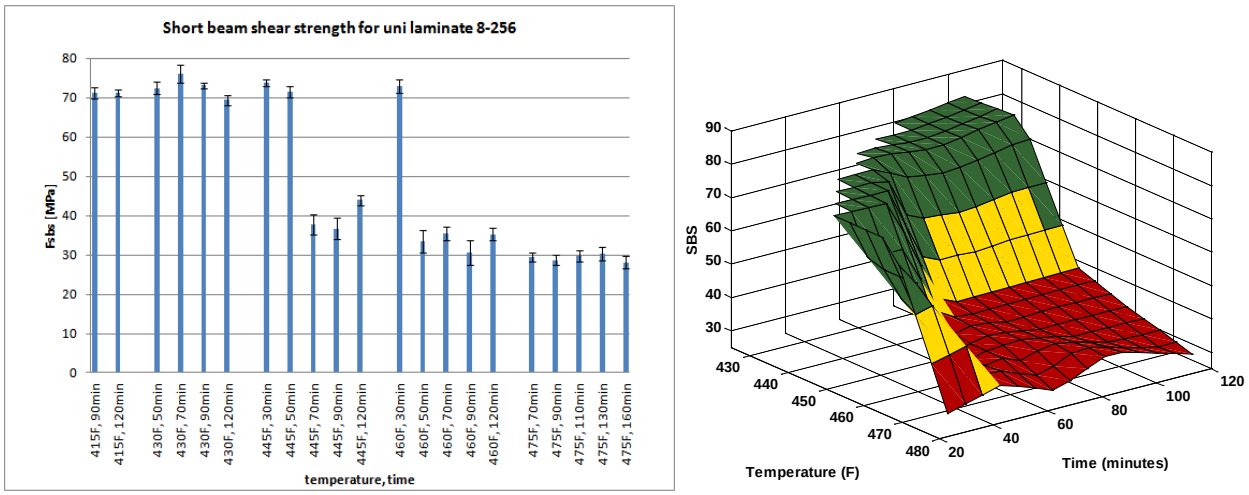

Figure 34. Force vs. Temperature/Time Combinations for BMS8-256 (4″ coupons)

The IR data were obtained on these BMS8-256 4″ coupons (figure 35) using the ExoScan system. The conditions for processing the IR data were the same as for the earlier work for 1″ coupons: the frequency range used was 1454 cm^{-1}-1197 cm^{-1}; the spectra were preprocessed via a second derivative (Savitzky-Golay 15 pt., second order) and normalized to unit length from 1954 cm^{-1}-725 cm^{-1}.

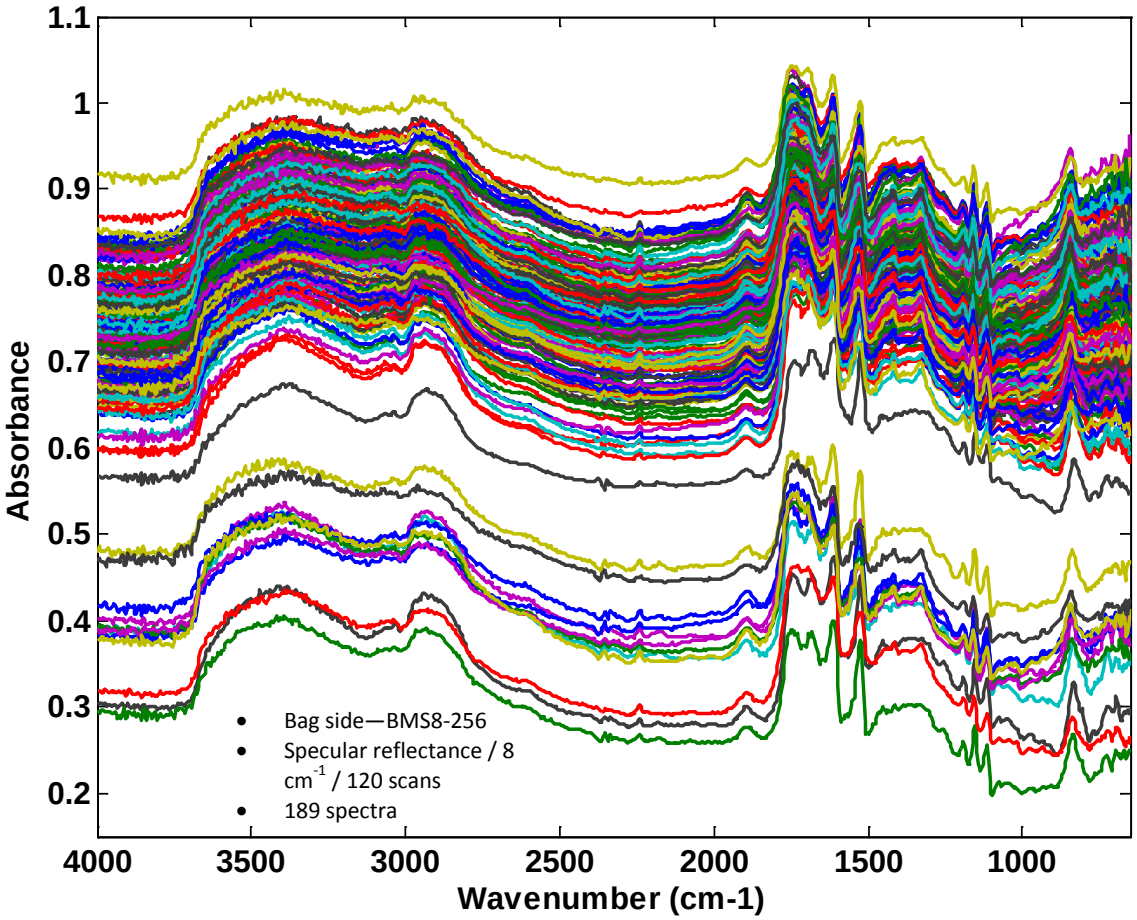

Figure 35. The IR Spectra for 4″ BMS8-256 Coupons

Similar to BMS8-276 coupons, there are three clusters (figure 36) representing the high-, medium-, and low-exposure levels for 4″ coupons.

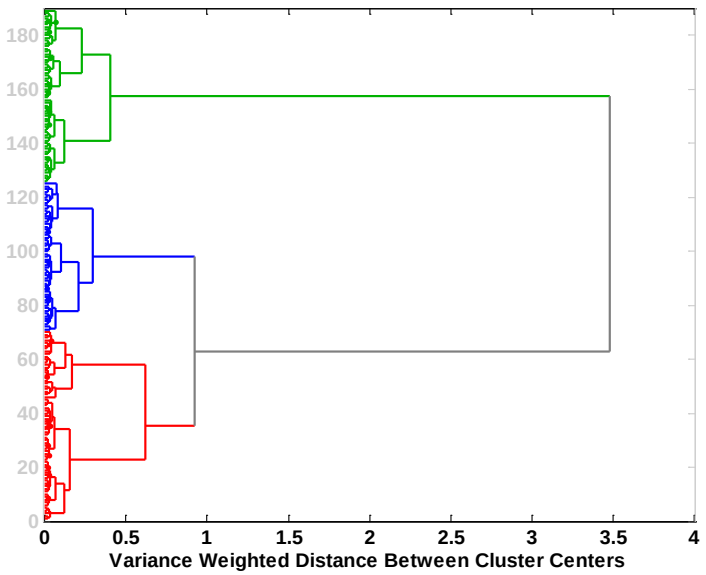

Figure 36. Cluster Analysis of Spectral Data for 4″ BMS8-256 Coupons

The colors of the second derivative spectra of the BMS8-256 samples (figure 37) are consistent with those used in figure 36.

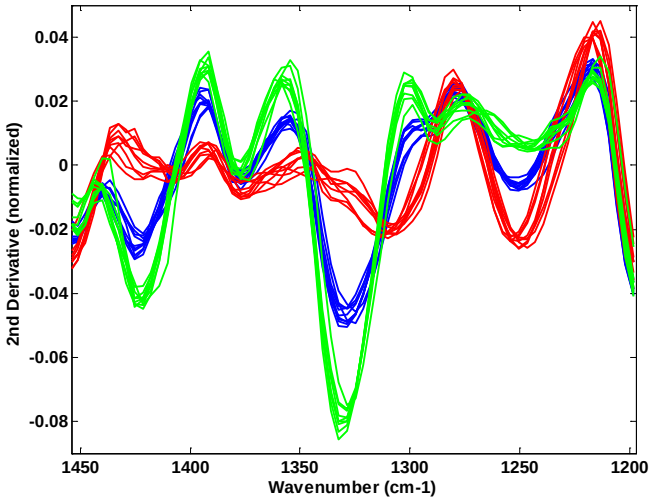

Figure 37. Second Derivative IR Spectra Demonstrating Clustering of Low, Medium, and High Exposure in the 4″ BMS8-256 Coupons: 430°F, 50 Minutes (red); 445°F, 120 Minutes (blue); 475°F, 120 Minutes (green)

The changes in second derivative spectra for the 4″ x 4″ BMS8-256 coupons exposed to 460°F for increasing amounts of time (figure 29) are indicative of chemical changes in the polymer backbone region that occur as the composite transitions from lower to higher levels of exposure.

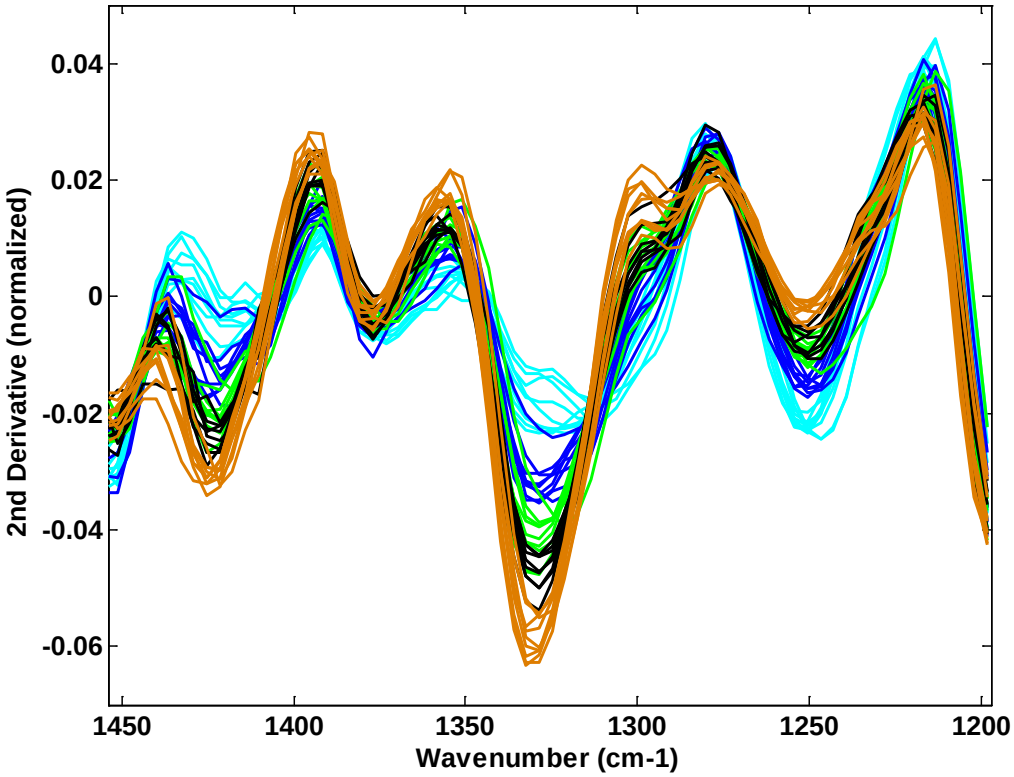

Figure 38. Second Derivative Spectra of 4″ BMS8-256 Composite Coupons Exposed to 460°F for Progressive Times – 30 Minutes (cyan), 50 Minutes (blue), 70 Minutes (green), 90 Minutes (black), and 120 Minutes (orange)

When the second derivative spectra of the 460°F exposed 4″ coupons are overlaid with those of the earlier 1″ coupons, which were treated with minimum and maximum temperature/time exposure, the data appear quite consistent (figures 38 and 39). The relative differences in the second derivative spectra band height reflect the degree of thermal exposure and confirm the capability of the FTIR measurement to detect progressive changes in the molecular structure of the composite.

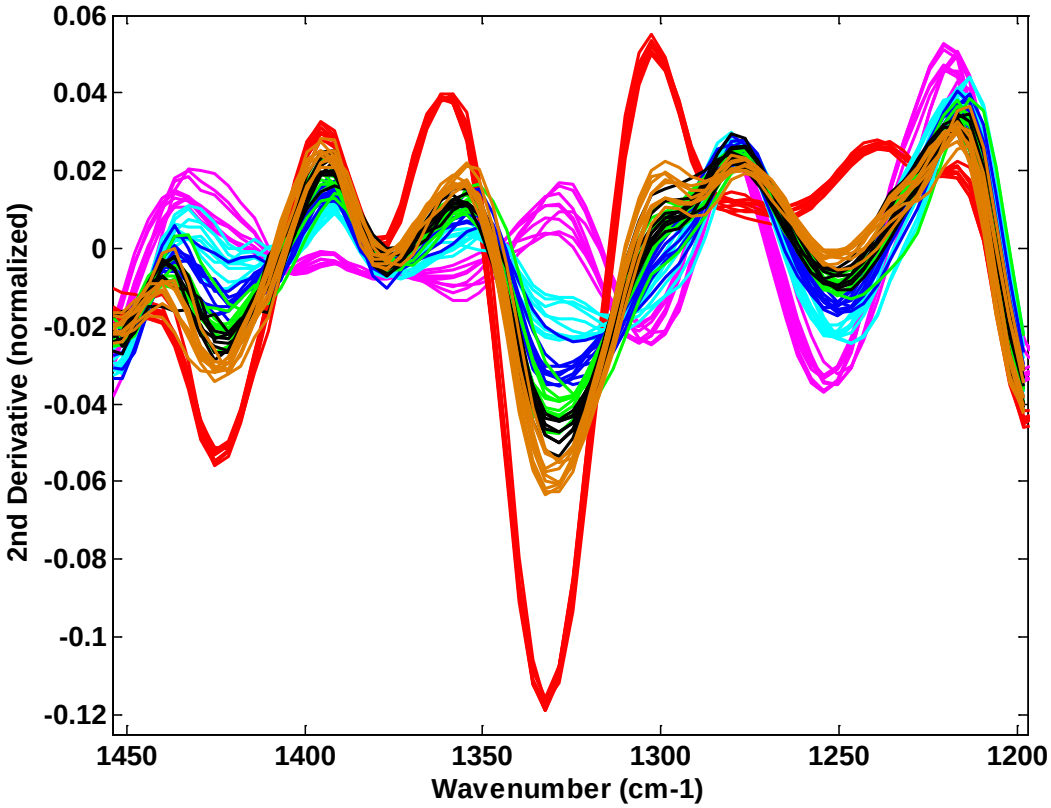

Figure 39. Second Derivative Spectra of 4″ BMS8-256 Composite Coupons Exposed to 460°F for Progressive Times – 30 Minutes (cyan), 50 Minutes (blue), 70 Minutes (green), 90 Minutes (black), and 120 Minutes (orange) Overlayed With Earlier 1″ Minimum (purple) and Maximum (red) Thermally Damaged Coupons

3.11 ULTRASOUND AND MICROSCOPY.

In general, little or no change in the ultrasound traces are observed for the lower temperature exposures relative to unexposed samples (figure 40). For longer exposure and higher temperature exposures, changes are observed. For example, in evaluation sample 17, A-scan measurements indicate that back surface reflection is delayed after exposure (figure 41). This could possibly be the result of delamination actually increasing the thickness of the sample. After longer exposure at elevated temperatures, the A-scan measurement (figure 42) shows significant attenuation of back surface reflection. The C-scan of gate 2 for this latter sample is quite different than for the other exposures (figure 43), with significant changes in back surface amplitude for sample 20 after exposure. Ultrasound measurements are able to detect changes in the composite for excessive thermal exposure (maximum exposure time and temperature). In this work, the technique appears to be relatively insensitive for detecting changes at less than the highest temperature and time combination, but further work is being done at AANC on this question. Microscopic examination of these composites are consistent with the ultrasound results (i.e., significant inter- and intralayer structural changes are observed (figure 44) as the exposure time and temperature increase).

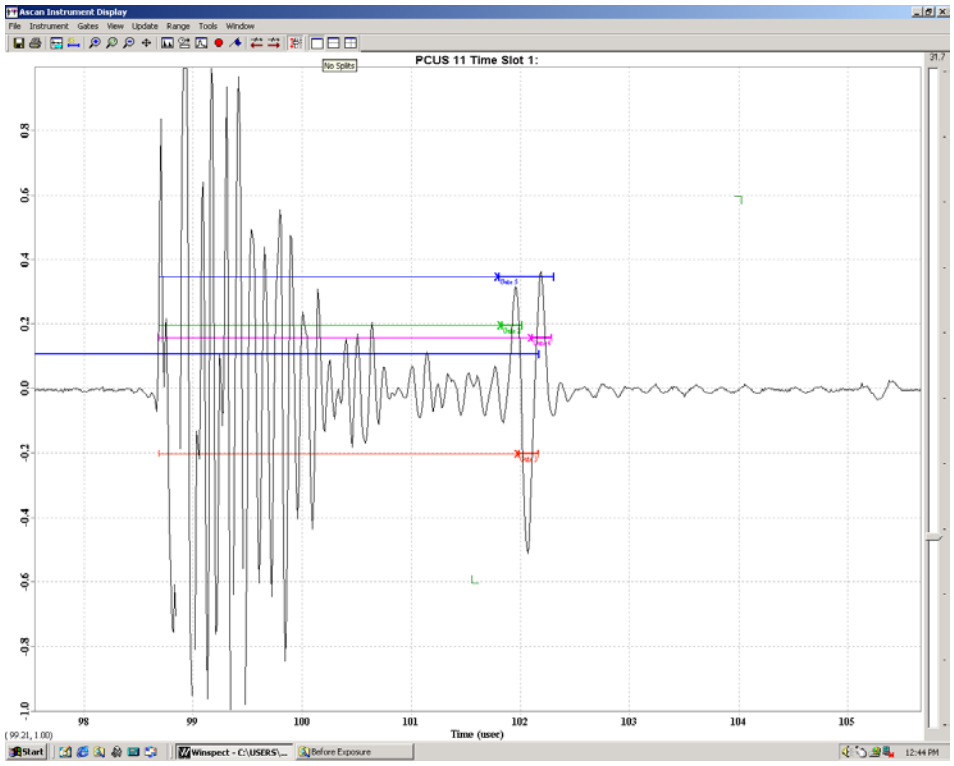

Figure 40. A-Scan Measurement of Composite Prior to Thermal Exposure

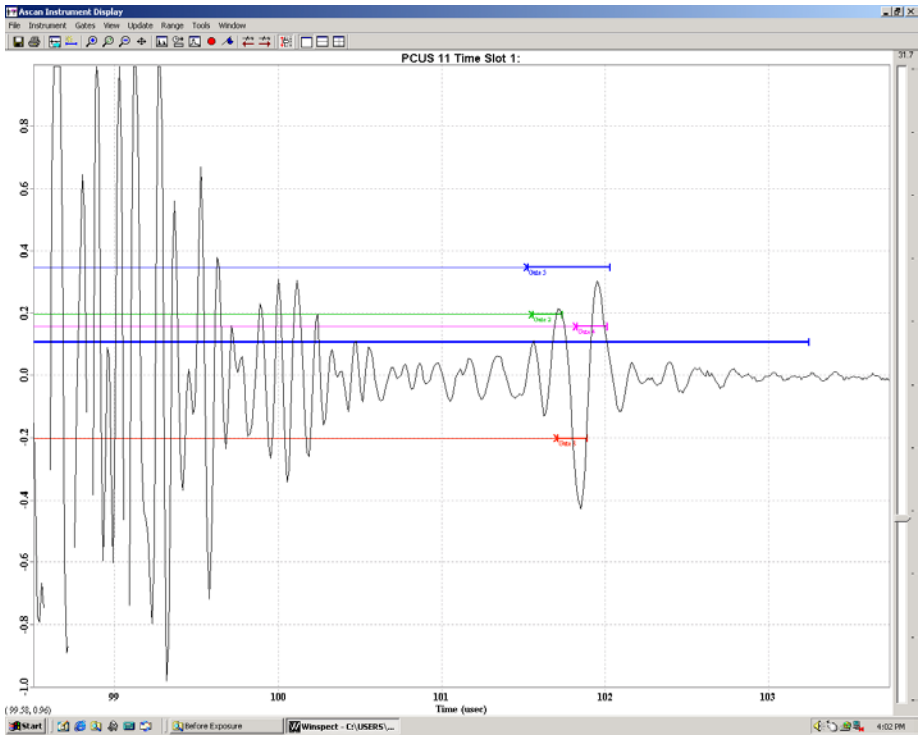

Figure 41. A-Scan Measurement of Composite After Thermal Exposure (445°F for 318 minutes)

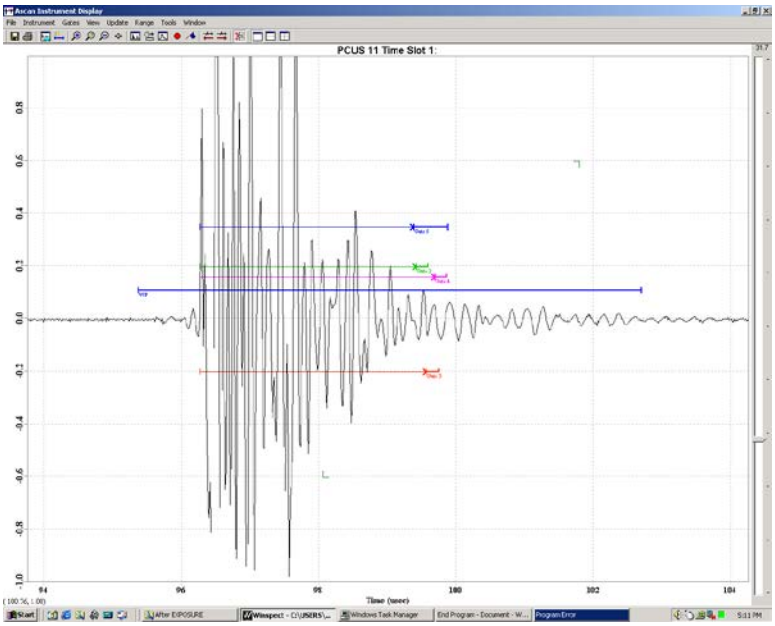

Figure 42. A-Scan Measurement of Composite After Thermal Exposure (445°F for 510 minutes)

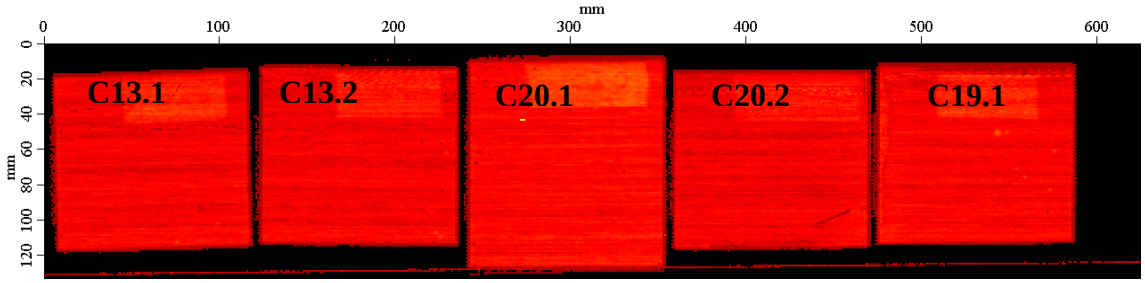

Prior to exposure

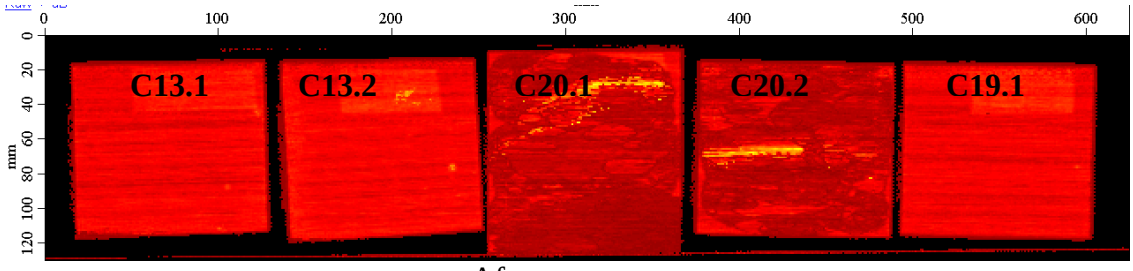

After exposure

Figure 43. C-Scan Measurements (Gate 02) of Composite Coupons: C13 Exposed to 385°F for 198 Minutes; C19 Exposed to 415°F for 510 Minutes; C20 Exposed to 445°F for 510 Minutes

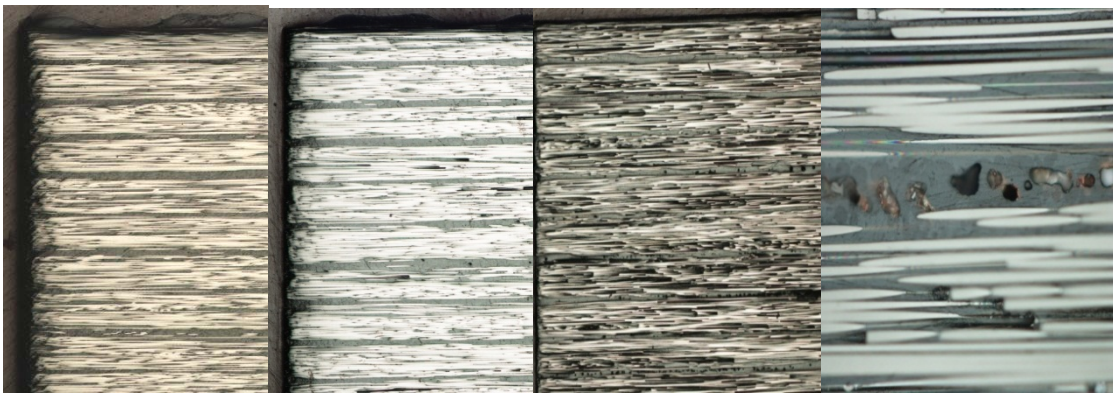

Low Exposure	Medium Exposure	High Exposure	High Exposure
415°F, 30 min	415°F, 200 min	535°F, 30 min	535°F, 30 min
5X	5X	5X	50X

Figure 44. Microscopic Evalution of BMS8-256 as a Function of Increasing Temperature and Exposure Time

Summaries of the evaluations of BMS8-256 (figure 45) and BMS8-276 (figure 46) show that changes in the mechanical strength of the composite as a function of thermal exposure are consistent with ultrasound results. This also corresponds to changes in the microstructure of the material, as indicated by visual micro-inspection.

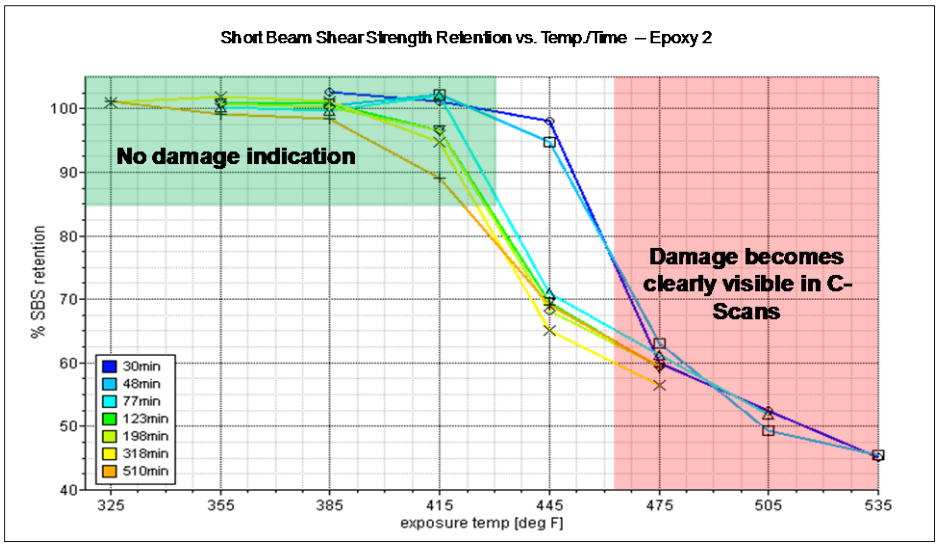

Figure 45. Summary of SBS, Ultrasound, and Microscopic Analysis of BMS8-256 Coupons as a Function of Temperature/Time Exposures

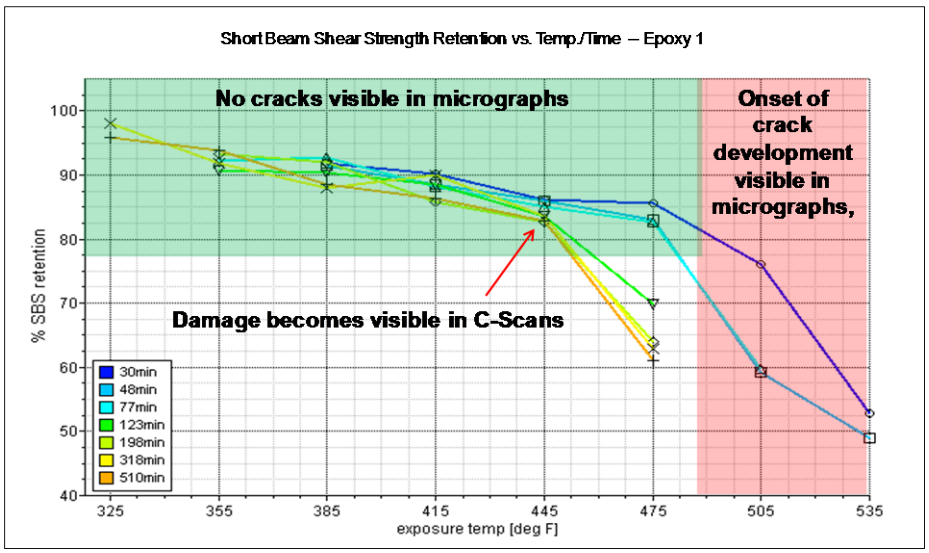

Figure 46. Summary of SBS, Ultrasound, and Microscopic Analysis of BMS8-276 Coupons as a Function of Temperature/Time Exposures

4. SUMMARY.

This research project characterized the capability of a handheld FTIR analyzer to measure thermally induced changes in aircraft composite. The overall objective was to assess the capabilities of a portable NDI technology that can elucidate incipient thermal damage by detecting changes in the molecular structure of the composite, which may precede the formation of micro-cracks or delaminations.

A summary of the actions, results, and conclusions of the project follows:

- A DoE was developed for thermal exposure that encompassed a range of times and temperatures reflecting potential real-world situations.

- BMS8-256 and BMS8-276 composite material, used in Boeing 787 and 777 aircraft, was provided by Boeing. Numerous coupons and panels were analyzed by FTIR, mechanical strength tests, ultrasound, and microscopy.

- Two sets of triplicate coupons were created for each time/temperature exposure combination on the two different composites. One set was used for FTIR measurement (nondestructive) and the other for SBS mechanical strength tests (destructive).

- The SBS measurements of the thermally exposed composite were carried out in triplicate for each of the representative time/temperature exposures. The SBS measurements showed a clear pattern of mechanical strength degradation and a fairly sharp transition from pristine composite to material that was affected by the thermal exposure.

- Extensive analysis of sanded and unsanded coupons was carried out by FTIR spectroscopy. The sanded coupons simulated composite under repair and had a higher ratio of carbon fiber to epoxy resin content than did the unsanded composite. Diffuse reflectance IR spectroscopy was found to give higher absorbance to noise (A/N) values for the sanded coupons than specular reflectance. Specular reflectance and diffuse reflectance provided similar A/N results for both sanded and unsanded composite coupons.

- As part of this research, a new high collection efficiency diffuse reflectance sampling interface was developed for the 4100 ExoScan FTIR system. The ExoScan equipped with the new diffuse sampling accessory was subsequently used for the FTIR analysis of composite coupons.

- Diffuse reflectance FTIR measurements of the thermally exposed composite were carried out in triplicate for each of the representative time/temperature exposures. These analyses showed the relationship between thermal exposure and changes in the molecular structure of the composite. Oxidation of the composite induced by heating was evidenced by the formation of a strong C=O absorbance band in the IR spectrum at approximately 1720 cm^{-1}.

- A PLS method was created to analyze the results of SBS and FTIR measurements. These measurements showed that changes in the mechanical strength and chemical bonding as a result of thermal exposure are well correlated. Diffuse reflectance FTIR measurement is largely a surface measurement (i.e., the diffusely scattered IR radiation that is collected from the composite represents information from the top 10 microns of the composite surface). Conversely, the mechanical strength measurement is of the bulk composite (i.e., it reflects the strength of the composite coupon that had a thickness of several thousand microns). The results obtained from the correlation of FTIR and SBS measurements indicate that the spectroscopic surface technique effectively mirrors strength changes occurring in the bulk material.

- Neural net and cluster analysis methods were also developed for the FTIR data and revealed clear patterns of change in the chemical structure of the composite as a function of thermal stress.

- A-scan and C-scan ultrasound measurements and optical microscopy were carried out on the composite samples. These revealed changes as a function of time/temperature exposure that were shown to be consistent with loss of mechanical strength and correlated well with the SBS results.

- When composite is exposed to thermal stress, the damage is often nonhomogeneous and extends in three dimensions. To repair this damage, a sanding and patching process may be used. It is necessary to define the shape and extent of the damage so that it can be removed prior to the repair. The handheld FTIR system was successfully used to define the extent of thermal damage in a series of 12″ x 12″ BMS8-256 and BMS8-276 composite panels that were intentionally heat damaged in irregular patterns. This was accomplished by mapping the height of the 1720 cm^{-1} C=O absorbance band, which is indicative of epoxy oxidation, as a function of distance.

- In a concurrent project with Boeing, thermally damaged composite coupons were prepared as validation standards for the 4100 ExoScan handheld FTIR. A calibration method for measuring composite thermal exposure is now available for the FTIR analyzer and a set of these validation standards is provided to users of the instrument [3]. The 4100 ExoScan FTIR system with aforementioned methods is now cited in the 787 Service Repair Manual in the NDT section [4]. A publication entitled "Complete System for Composite Measurements on Boeing 787 Aircraft" is available from Agilent Technologies.

- As of the time of this report, several airlines and aircraft maintenance organizations have acquired the ExoScan system and the validation standards for use with Boeing 787 aircraft [5]. Moreover, other aircraft and aircraft part manufacturers are also involved in projects to use the ExoScan FTIR system with their composite-based materials.

5. CONCLUSIONS.

Fourier Transform Infrared Spectroscopy (FTIR) molecular analysis effectively correlates with the results of destructive mechanical strength tests and adequately reflects changes in the composite material, which occur as a function of thermal exposure. The FTIR measurements are shown to be progressively sensitive and, thus, can be helpful in detecting incipient thermal damage. The FTIR system can be used to map the breadth and depth of thermal exposure in a suspect portion in support of sanding and repair processes. The method that has been developed for tracking this damage has been incorporated into the 4100 ExoScan FTIR software and it has been shown that a trained nondestructive testing (NDT) technician can effectively use the system.

The recent availability of handheld FTIR analyzers comes at an opportune time with respect to the increasing use of composite in civilian aircraft. The ability to nondestructively analyze the integrity of the chemical and molecular structure of these organic-based materials provides a needed NDT capability. Based on the results of this project, it appears that portable FTIR can provide useful information in support of the manufacturing and maintenance of composite-based aircraft.

6. REFERENCES.

1. Williams, J.H., "Crash Should Prompt a Change in Composite Inspection Philosophy," Air Safety Week, July 29, 2002.

2. Janke, J.C., Wachter, E.A., Philpot, H.E, and Powell, G.L., "Composite Heat Damage Assessment," Oak Ridge National Laboratory, 1990.

3. Seelenbinder, J., "Composite Heat Damage Measurement Using the Handheld Agilent 4100 ExoScan FTIR," Agilent Technologies Application Note, Available at http://www.chem.agilent.com/Library/applications/5990-7798EN.pdf, Accessed September 4, 2014.

4. The Boeing Company, "Boeing 787 NDT Manual Part 9," 51-00-03, 2011.

5. Arnaud, C.H., "Handheld IR in the Hangar," *Chemical and Engineering News*, Vol. 89, No. 34, 2011, pp. 43-45.